

Beyond the Standard Model Physics and Precision Electroweak Measurements at the EIC

Sonny Mantry

University of North Georgia (UNG)

*ePIC, Collaboration Meeting
January 11th, 2022*

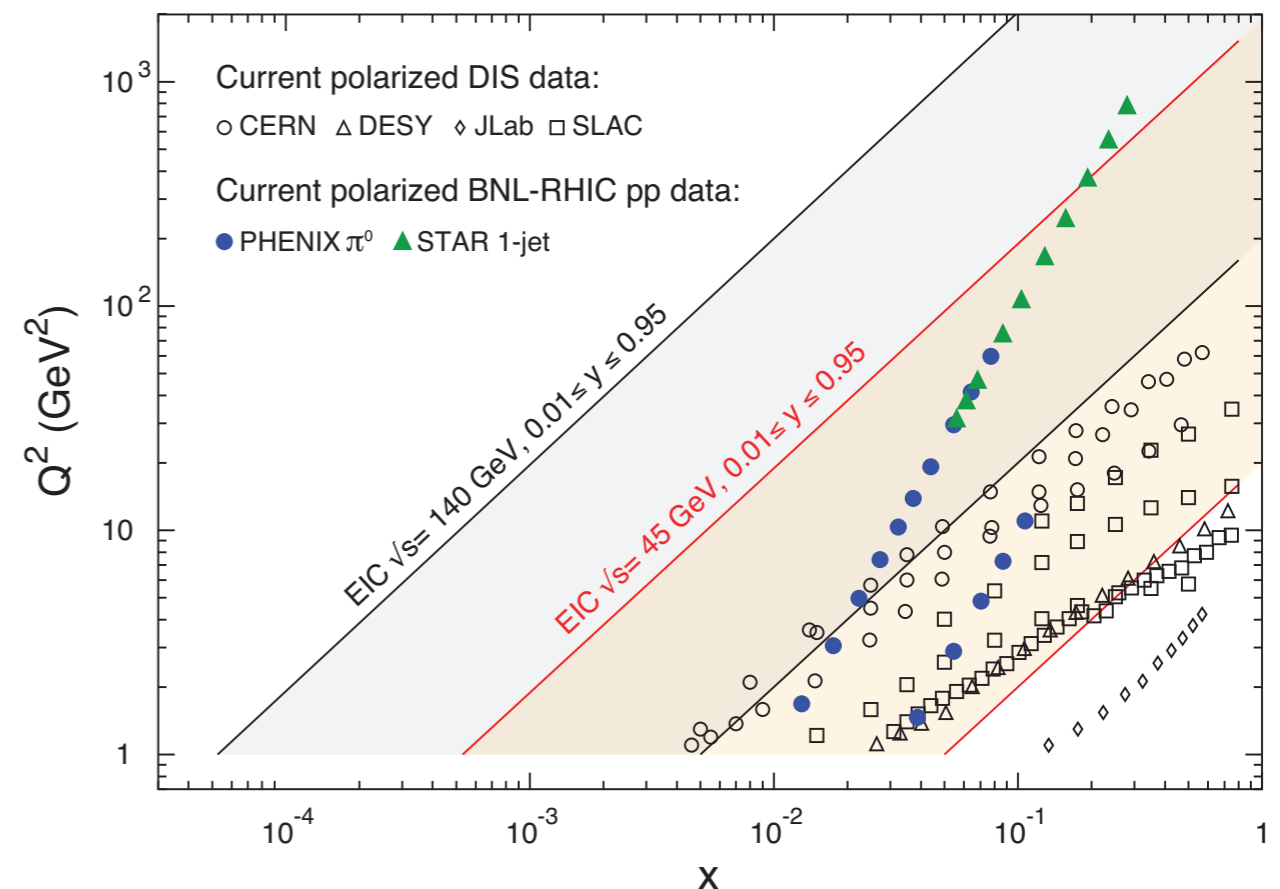
Physics Beyond the Standard Model at the EIC

- The EIC is primarily a QCD machine.
- However, the EIC can also constrain BSM and be complementary to LHC searches and constraints from other low energy experiments:

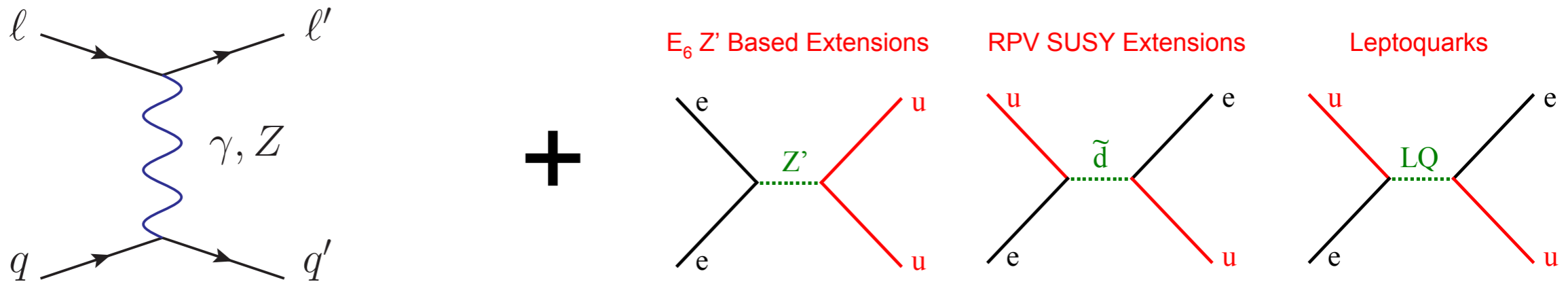
- Precision measurements of the electroweak parameters
 - Leptophobic Z'
 - Dark Photon
 - Dark Z
- SMEFT Analysis to Constrain BSM
- Charged Lepton Flavor Violation

- Such a physics program is facilitated by:

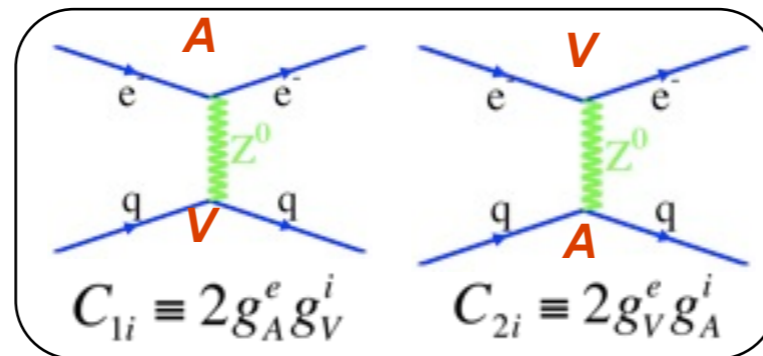
- high luminosity
- wide kinematic range
- range of nuclear targets
- polarized beams
- Variety of observables



Neutral Current DIS



- Cross section asymmetries in neutral current DIS can probe BSM physics beyond the electroweak scale.
- The parity-violating SM contributions depend on the C_{1q} and C_{2q} couplings as shown



- Tree-level Standard Model values:

$$C_{1u} = -\frac{1}{2} + \frac{4}{3} \sin^2(\theta_W), \quad C_{2u} = -\frac{1}{2} + 2 \sin^2(\theta_W), \quad C_{3u} = \frac{1}{2},$$

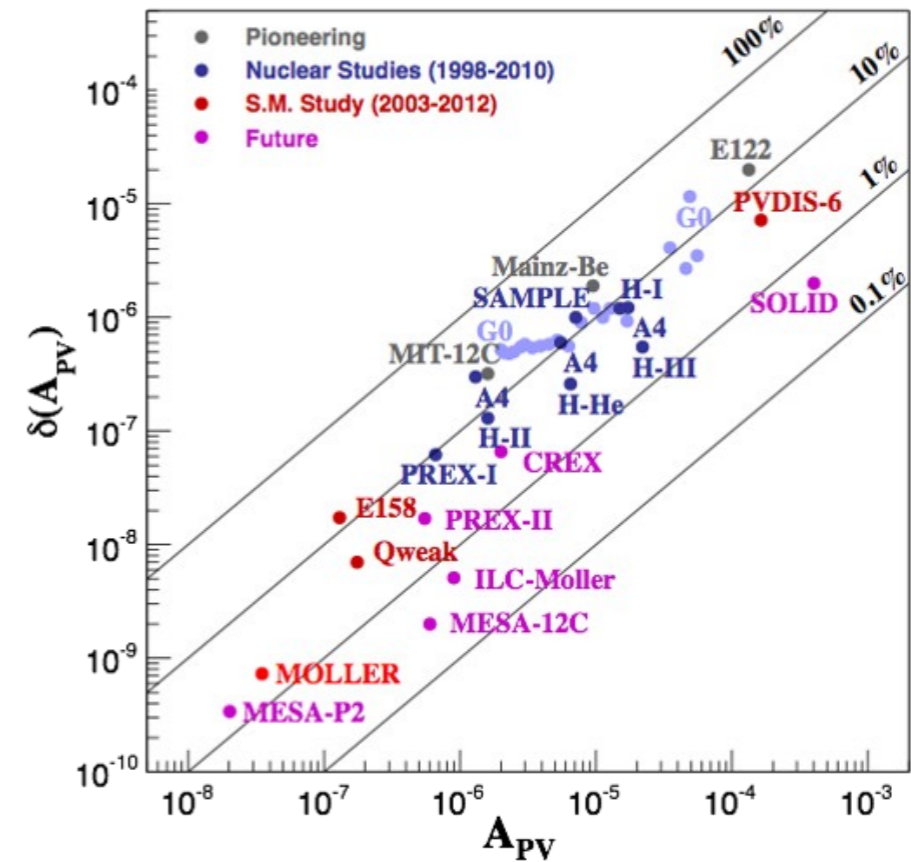
$$C_{1d} = \frac{1}{2} - \frac{2}{3} \sin^2(\theta_W), \quad C_{2d} = \frac{1}{2} - 2 \sin^2(\theta_W), \quad C_{3d} = -\frac{1}{2}$$

- Precision measurements of the weak mixing angle can probe BSM physics.

Accessing C_{iq} via Parity-Violating Observables

- Atomic Parity Violation (APV):
Sensitive to C_{1q} couplings via $Q_W(Z, N)$
- Parity Violating Elastic Scattering (Qweak, P2):
Sensitive to C_{1q} couplings through $Q_W(Z = 1, N = 0)$

$$Q_W(Z, N) = -2[C_{1u}(2Z + N) + C_{1d}(Z + 2N)]$$

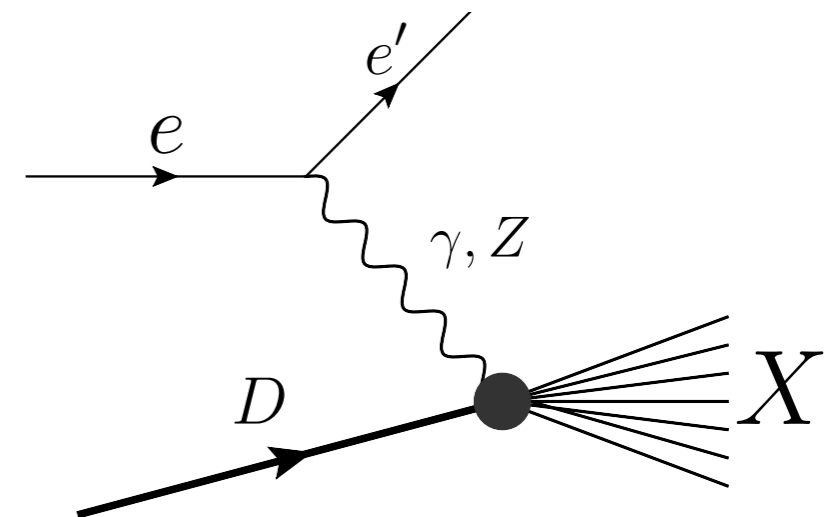


- Parity Violating DIS (E122, PVDIS-6, SOLID, EIC):
Sensitive to C_{1q} and C_{2q}

$$A_{PV}^{DIS} = \frac{G_F Q^2}{4\sqrt{2}(1 + Q^2/M_Z^2)\pi\alpha} \left[a_1 + \frac{1 - (1 - y)^2}{1 + (1 - y)^2} a_3 \right]$$

$$a_1 = \frac{2 \sum_q e_q C_{1q}(q + \bar{q})}{\sum_q e_q^2 (q + \bar{q})} \quad a_3 = \frac{2 \sum_q e_q C_{2q}(q - \bar{q})}{\sum_q e_q^2 (q + \bar{q})}$$

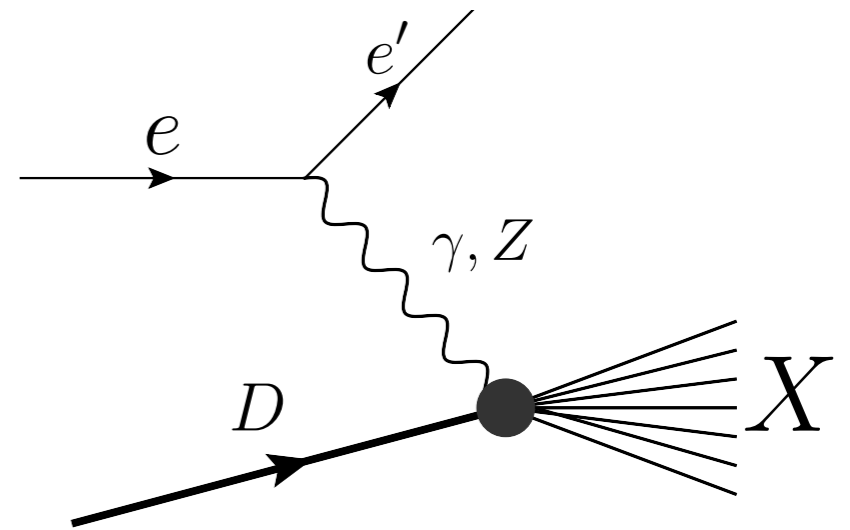
For the isoscalar deuteron target,
structure function effects largely cancel



Parity-Violating e-D Asymmetry

- Parity-violating e-D asymmetry is a powerful probe of the WNC couplings:

$$A_{\text{PV}} \equiv \frac{\sigma_R - \sigma_L}{\sigma_R + \sigma_L} \simeq \frac{|A_Z|}{|A_\gamma|} \simeq \frac{G_F Q^2}{4\pi\alpha} \simeq 10^{-4} Q^2$$



- Due to the isoscalar nature of the Deuteron target, the dependence of the asymmetry on the structure functions largely cancels (Cahn-Gilman formula).

$$A_{\text{CG}}^{\text{RL}} = -\frac{G_F Q^2}{2\sqrt{2}\pi\alpha} \frac{9}{10} \left[\left(1 - \frac{20}{9} \sin^2 \theta_W\right) + \left(1 - 4 \sin^2 \theta_W\right) \frac{1 - (1 - y)^2}{1 + (1 - y)^2} \right]$$



- e-D asymmetry allows a precision measurement of the weak mixing angle.

Corrections to Cahn-Gilman

- Hadronic effects appear as corrections to the Cahn-Gilman formula:

$$A_{RL} = -\frac{G_F Q^2}{2\sqrt{2}\pi\alpha} \frac{9}{10} \left[\tilde{a}_1 + \tilde{a}_2 \frac{1 - (1 - y)^2}{1 + (1 - y)^2} \right]$$

$$\tilde{a}_j = -\frac{2}{3} (2C_{ju} - C_{jd}) [1 + R_j(\text{new}) + R_j(\text{sea}) + R_j(\text{CSV}) + R_j(\text{TMC}) + R_j(\text{HT})]$$

↑
New physics

↑
Sea quarks

↑
Charge symmetry
violation

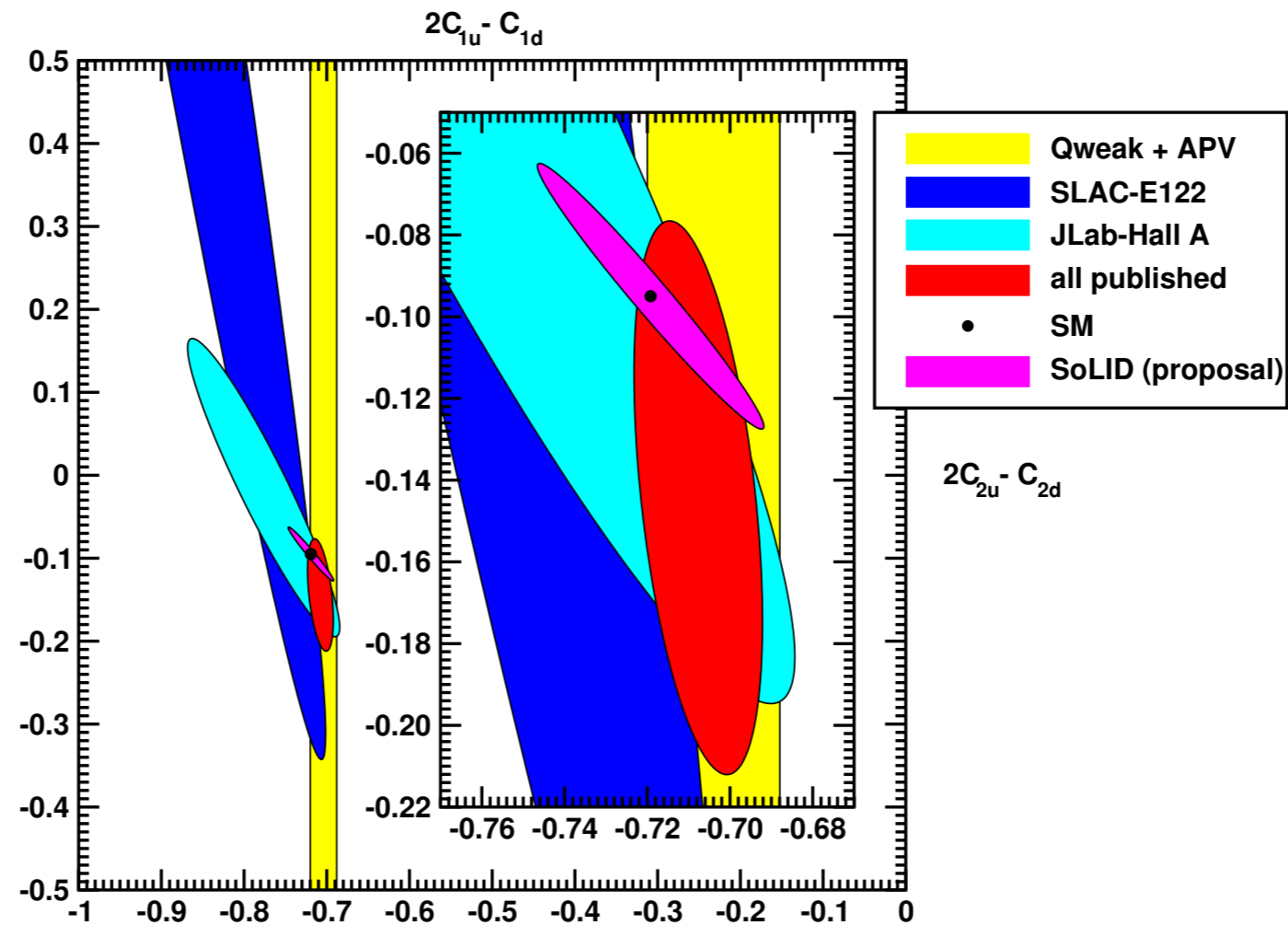
↑
Target mass

↑
Higher
twist

- Hadronic effects must be well understood before any claim for evidence of new physics can be made.

[Bjorken, Hobbs, Melnitchouk;
SM, Ramsey-Musolf, Sacco;
Belitsky, Mashanov, Schafer;
Seng, Ramsey-Musolf,]

Status of WNC Couplings



- The combination $2C_{1u} - C_{1d}$ is severely constrained by Qweak and Atomic Parity violation.
- The combination $2C_{2u} - C_{2d}$ is known to within $\sim 50\%$ from the JLAB 6 GeV experiment:

$$2C_{2u} - C_{2d} = -0.145 \pm 0.068$$

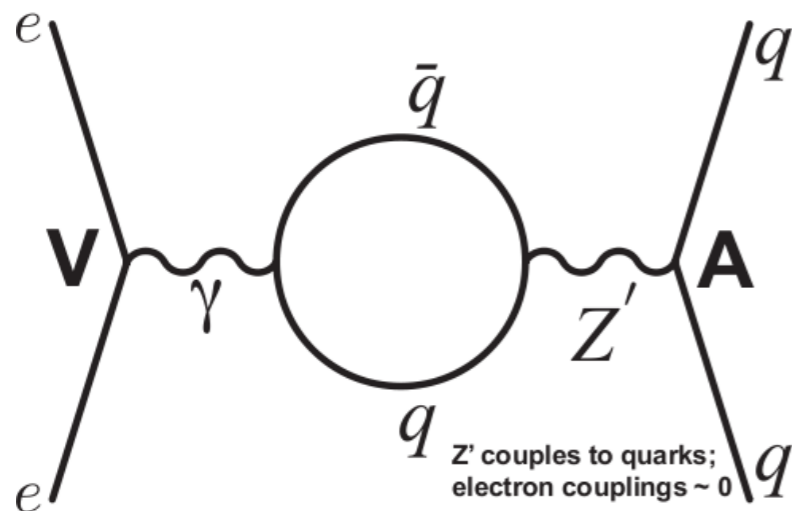
- SOLID is expected significantly improve on this result.
- The EIC can provide additional data from previously unexplored Q^2 range between fixed target and collider experiments

BSM Physics Scenarios

Leptophobic Z'

- Leptophobic Z's are an interesting BSM scenario since they only shifts the C_{2q} couplings in A_{PV}

- Leptophobic Z's only affect the $b(x)$ term or the C_{2q} coefficients in A_{PV} :



Leptophobic Z'
 contributes only to
 the C_{2q} couplings!

[M.Alonso-Gonzalez, M.Ramsey-Musolf;
 M.Buckley, M.Ramsey-Musolf]

$$A_{PV}^{\text{DIS}} = \frac{G_F Q^2}{4\sqrt{2}(1 + Q^2/M_Z^2)\pi\alpha} \left[a_1 + \frac{1 - (1 - y)^2}{1 + (1 - y)^2} a_3 \right]$$

Probing the Dark Sector

- Strong evidence for dark matter through gravitational effects:

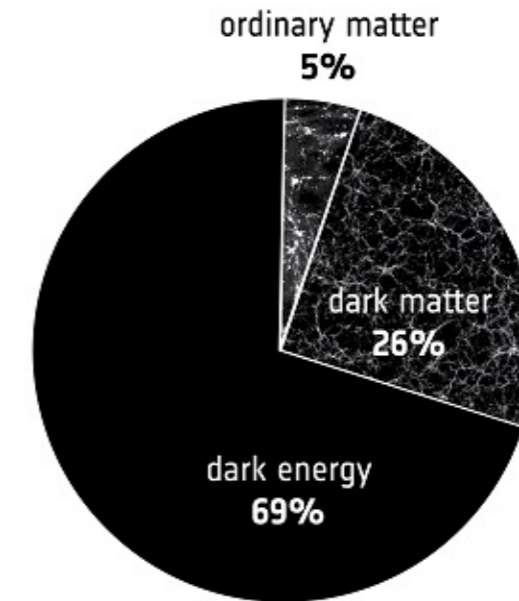
- Galactic Rotation Curves
- Gravitational Lensing
- Cosmic Microwave Background
- Large Scale Structure Surveys

- WIMP dark matter paradigm

- Mass \sim TeV
- Weak interaction strength couplings
- Gives the required relic abundance

- However, so far no direct evidence for WIMP dark matter

- Perhaps dark sector has a rich structure including different species and gauge forces, just like the visible sector



Dark Photon Scenario

- Dark $U(1)_d$ gauge group
- Interacts with SM via kinetic mixing (and mass mixing)

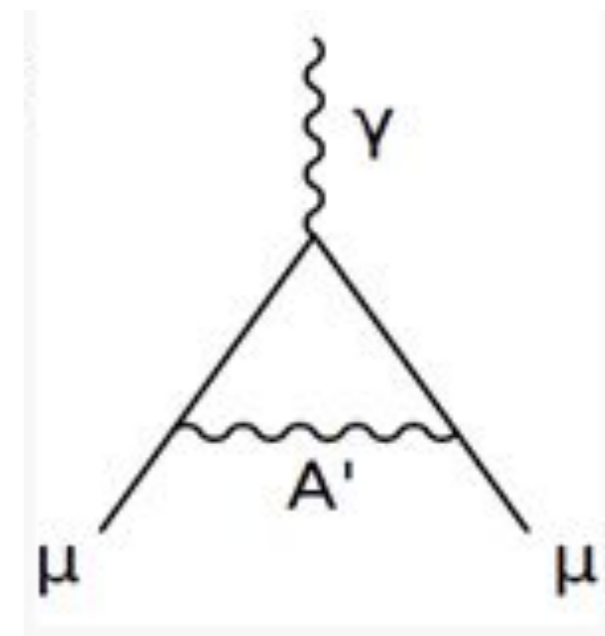
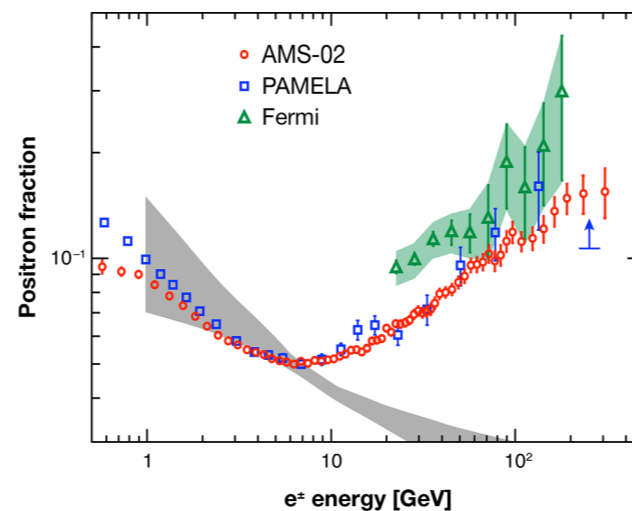
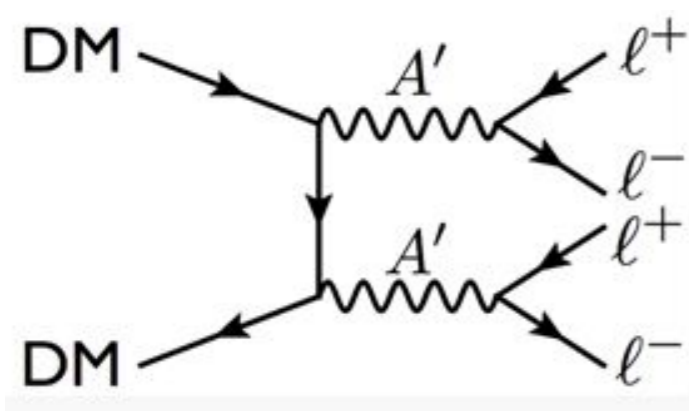
$$\mathcal{L} \supset -\frac{1}{4} F'_{\mu\nu} F'^{\mu\nu} + \frac{m_{A'}^2}{2} A'_\mu A'^\mu + \frac{\epsilon}{2 \cos \theta_W} F'_{\mu\nu} B^{\mu\nu}$$

- The mixing induces a coupling of the dark photon to the electromagnetic and weak neutral currents.

$$\mathcal{L}_{int} = -e\epsilon J_{em}^\mu A'_\mu$$

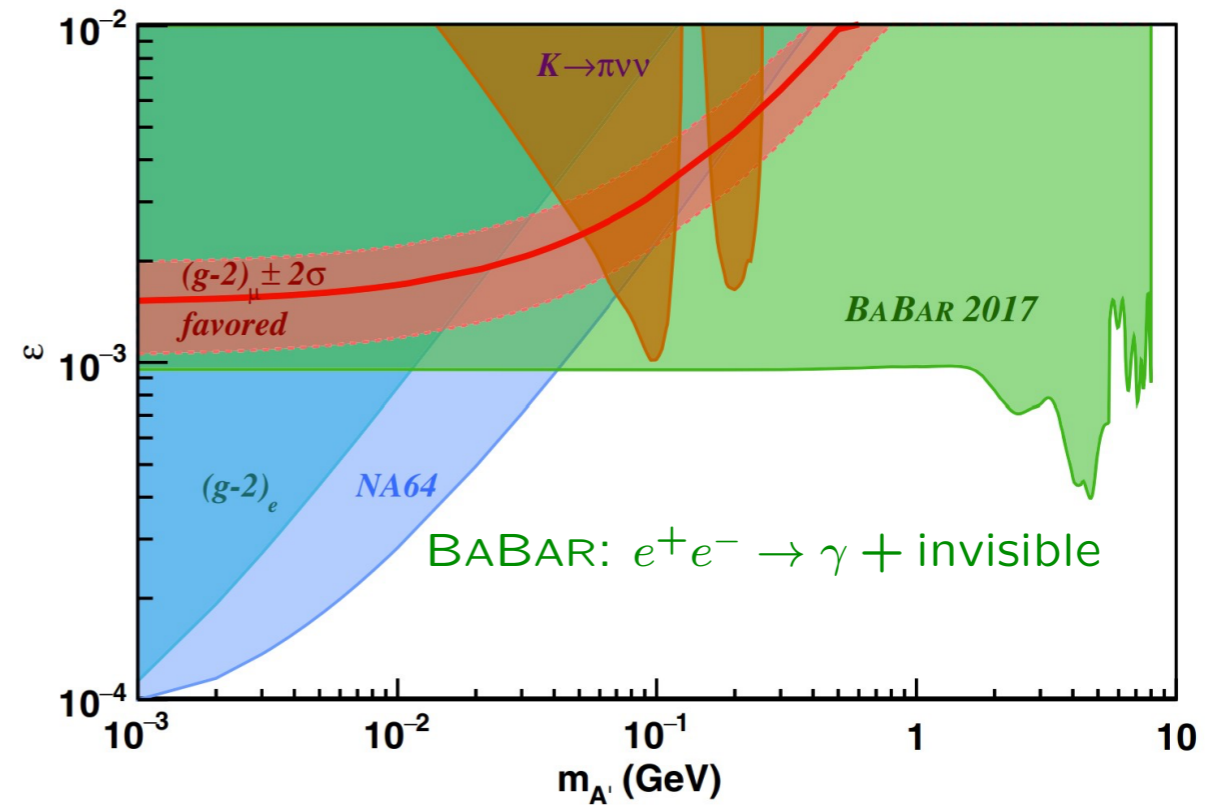
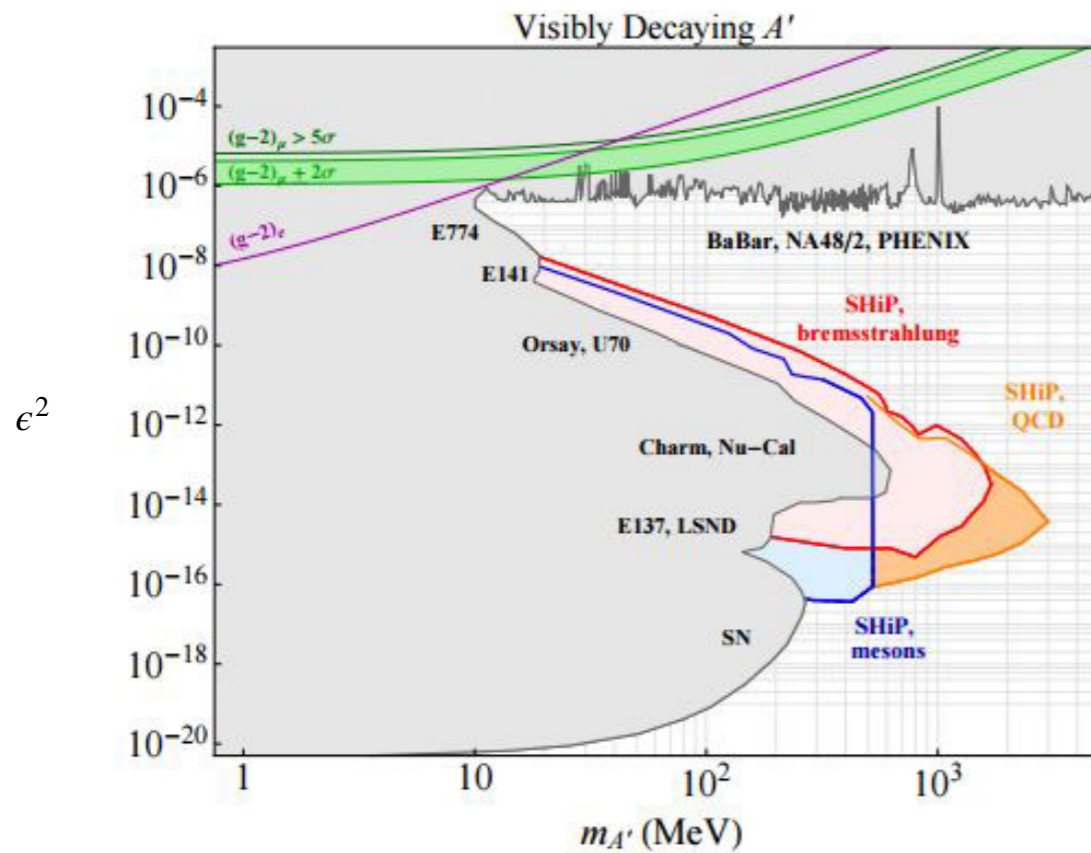
- Could help explain astrophysical data and anomalies

[Arkani-Hamed, Finkbeiner, Slatyer, Wiener, ...]



Dark Photon Scenario

- Active experimental program to search for dark photons
 [Bjorken, Essig, Schuster, Toro; Baten, Pospelov, Ritz; Izaguirre Krnjaic, Schuster, Toro]



S. Alekhin *et al.*, arXiv:1504.04855 [hep-ph]

Dark Photon Scenario: Impact on PVES

[Thomas, Wang, Williams]

$$\mathcal{L} \supset -\frac{1}{4}F'_{\mu\nu}F'^{\mu\nu} + \frac{m_{A'}^2}{2}A'_\mu A'^\mu + \frac{\epsilon}{2\cos\theta_W}F'_{\mu\nu}B^{\mu\nu}$$

- Constraints on Dark Photon parameter space will be independent of the details of the decay branching fractions of the dark photon
- For a light dark photon ($m_{A'} < 10 \text{ GeV}$), the induced coupling to the weak neutral current is suppressed (due to a cancellation between the kinetic and mass mixing induced couplings). [Gopalakrishna, Jung, Wells; Davoudiasl, Lee, Marciano]
- A heavier dark photon for a sizable coupling to the weak neutral current and a correspondingly sizable effect in PVES was recently considered. [Thomas, Wang, Williams]

Dark Photon Scenario: Impact on PVES

[Thomas, Wang, Williams]

$$\mathcal{L} \supset -\frac{1}{4}F'_{\mu\nu}F'^{\mu\nu} + \frac{m_{A'}^2}{2}A'_\mu A'^\mu + \frac{\epsilon}{2\cos\theta_W}F'_{\mu\nu}B^{\mu\nu}$$

- Constraints on Dark Photon parameter space will be independent of the details of the decay branching fractions of the dark photon
- Constraints on Dark Photon parameter space will be independent of the details of the decay branching fractions of the dark photon
- The usual PVDIS asymmetry has the form:

$$A_{\text{PV}}^{\text{DIS}} = \frac{G_F Q^2}{4\sqrt{2}(1 + Q^2/M_Z^2)\pi\alpha} \left[a_1 + \frac{1 - (1 - y)^2}{1 + (1 - y)^2} a_3 \right]$$

- Including the effects of a dark photon, we get additional terms:

$$A_{\text{PV}} = \frac{Q^2}{2\sin^2 2\theta_W (Q^2 + M_Z^2)} \left[a_1^{\gamma Z} + \frac{1 - (1 - y)^2}{1 + (1 - y)^2} a_3^{\gamma Z} \right. \\ \left. + \frac{Q^2 + M_Z^2}{Q^2 + M_{A_D}^2} \left(a_1^{\gamma A_D} + \frac{1 - (1 - y)^2}{1 + (1 - y)^2} a_3^{\gamma A_D} \right) \right],$$

Dark Photon Scenario: Impact on PVES

- Equivalent to working with the usual PVDIS formula:

$$A_{\text{PV}}^{\text{DIS}} = \frac{G_F Q^2}{4\sqrt{2}(1 + Q^2/M_Z^2)\pi\alpha} \left[a_1 + \frac{1 - (1 - y)^2}{1 + (1 - y)^2} a_3 \right]$$

- But with shifted C_{iq} couplings:

$$C_{1q} = C_{1q}^Z + \frac{Q^2 + M_Z^2}{Q^2 + M_{A_D}^2} C_{1q}^{A_D} = C_{1q}^{\text{SM}} (1 + R_{1q})$$

$$C_{2q} = C_{2q}^Z + \frac{Q^2 + M_Z^2}{Q^2 + M_{A_D}^2} C_{2q}^{A_D} = C_{2q}^{\text{SM}} (1 + R_{2q})$$

[Thomas, Wang, Williams]

Dark Photon Scenario: Shift in C_{iq} (PVDIS, HERA) [Thomas, Wang, Williams]

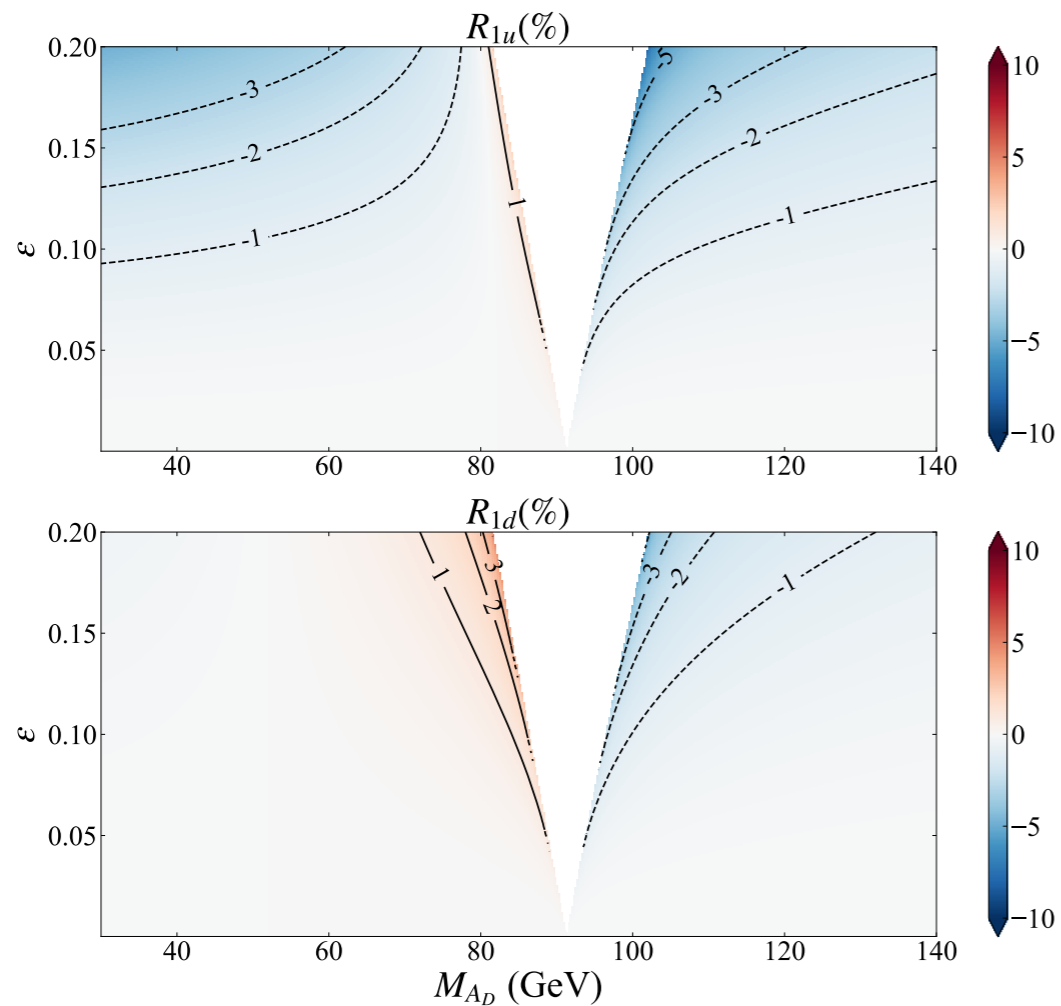


FIG. 2. The correction factors R_{1u} and R_{1d} at $Q^2 = M_Z^2$.

$$C_{1q} = C_{1q}^Z + \frac{Q^2 + M_Z^2}{Q^2 + M_{A_D}^2} C_{1q}^{A_D} = C_{1q}^{\text{SM}} (1 + R_{1q})$$

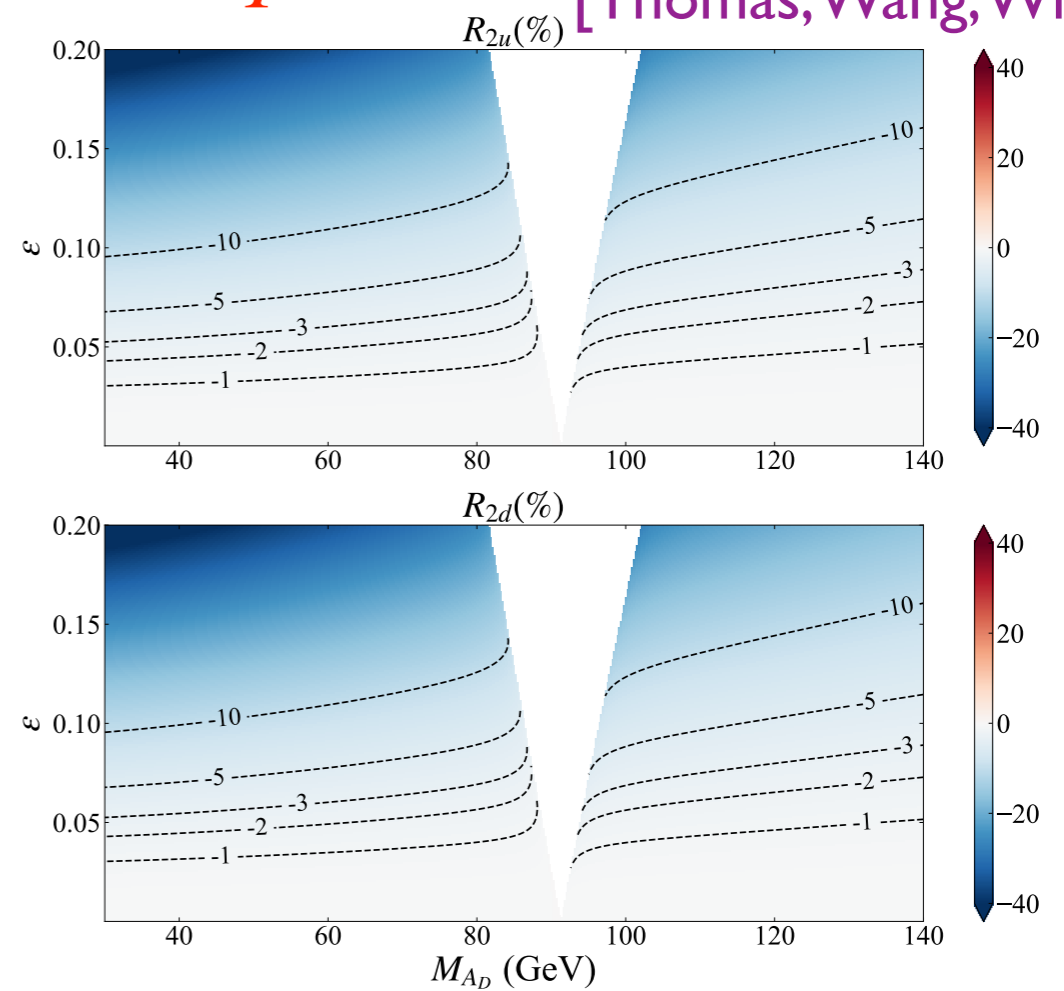


FIG. 3. The correction factors R_{2u} and R_{2d} at $Q^2 = M_Z^2$.

$$C_{2q} = C_{2q}^Z + \frac{Q^2 + M_Z^2}{Q^2 + M_{A_D}^2} C_{2q}^{A_D} = C_{2q}^{\text{SM}} (1 + R_{2q})$$

- Study could be easily extended to EIC kinematics.

Dark Photon Scenario: Shift in C_{iq} (PVDIS)

Qualitatively different behavior in shifts to C_{iq} for different Q^2

Useful to explore dark-photon space over a wide range of Q^2

Light Dark-Z Parity Violation

[Davoudiasl, Lee, Marciano]

- An interesting scenario is that of a “light” Dark-Z.

- The standard kinetic mixing scenario:

$$\mathcal{L}_{\text{gauge}} = -\frac{1}{4}B_{\mu\nu}B^{\mu\nu} + \frac{1}{2}\frac{\varepsilon}{\cos\theta_W}B_{\mu\nu}Z_d^{\mu\nu} - \frac{1}{4}Z_{d\mu\nu}Z_d^{\mu\nu}$$

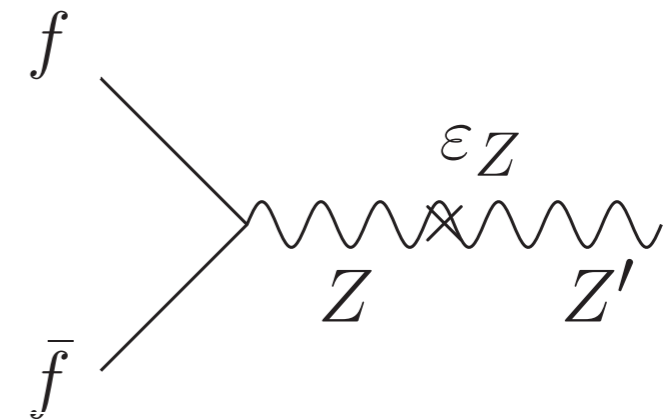
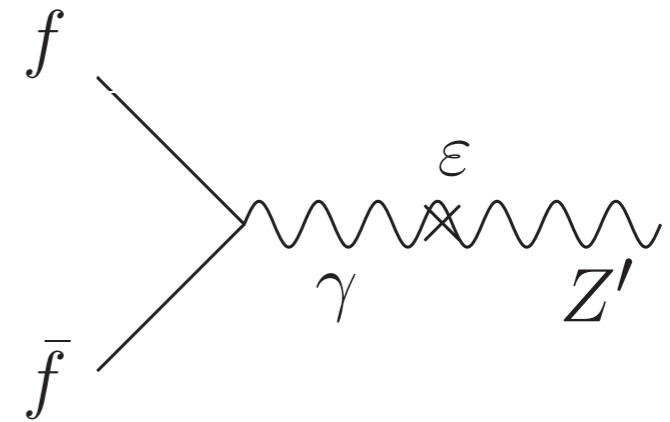
- And additional mass mixing (for example, from extended Higgs sector) can induce sizable dark-Z coupling to the weak neutral current:

$$M_0^2 = m_Z^2 \begin{pmatrix} 1 & -\varepsilon_Z \\ -\varepsilon_Z & m_{Z_d}^2/m_Z^2 \end{pmatrix}$$

$$\varepsilon_Z = \frac{m_{Z_d}}{m_Z} \delta$$

- Dark-Z couples to the electromagnetic and neutral current coupling:

$$\mathcal{L}_{\text{int}} = \left(-e\varepsilon J_\mu^{\text{em}} - \frac{g}{2\cos\theta_W}\varepsilon_Z J_\mu^{\text{NC}} \right) Z_d^\mu$$



Light Dark-Z Parity Violation

[Davoudiasl, Lee, Marciano]

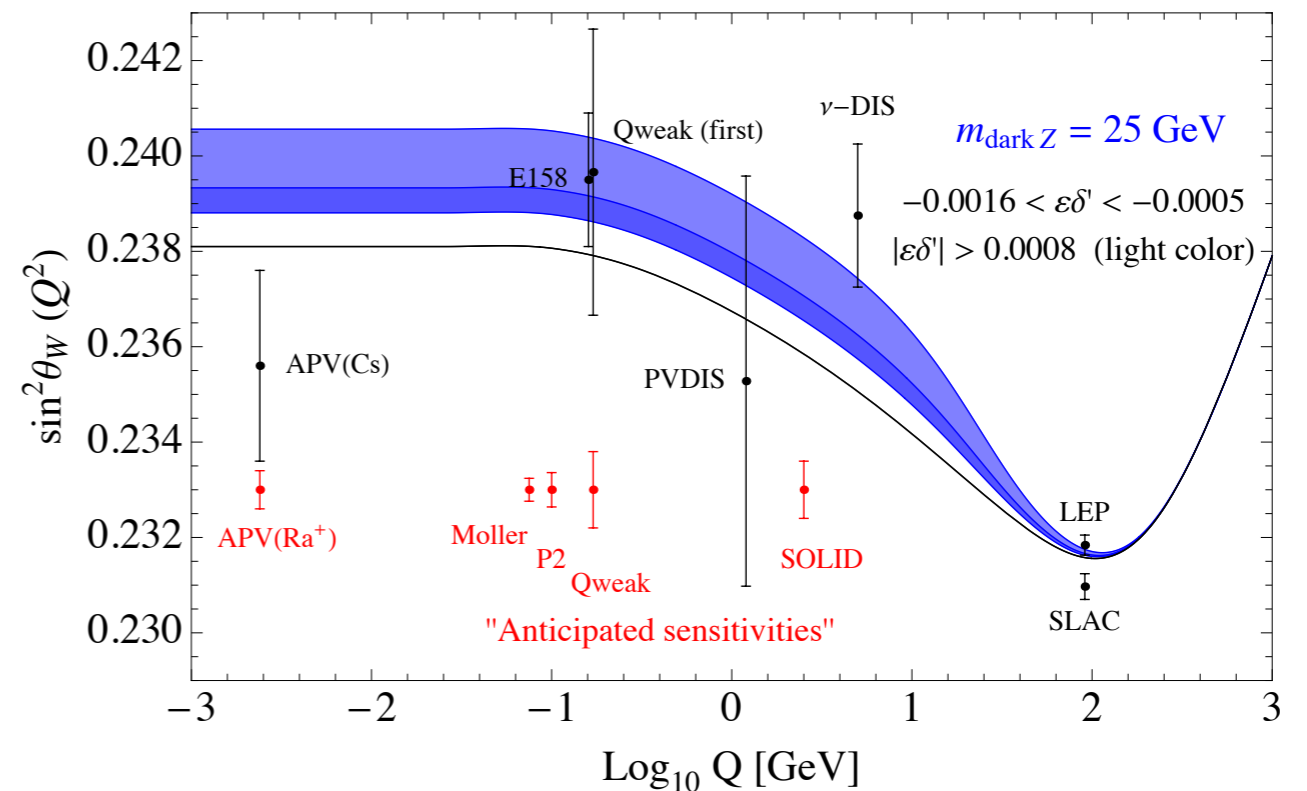
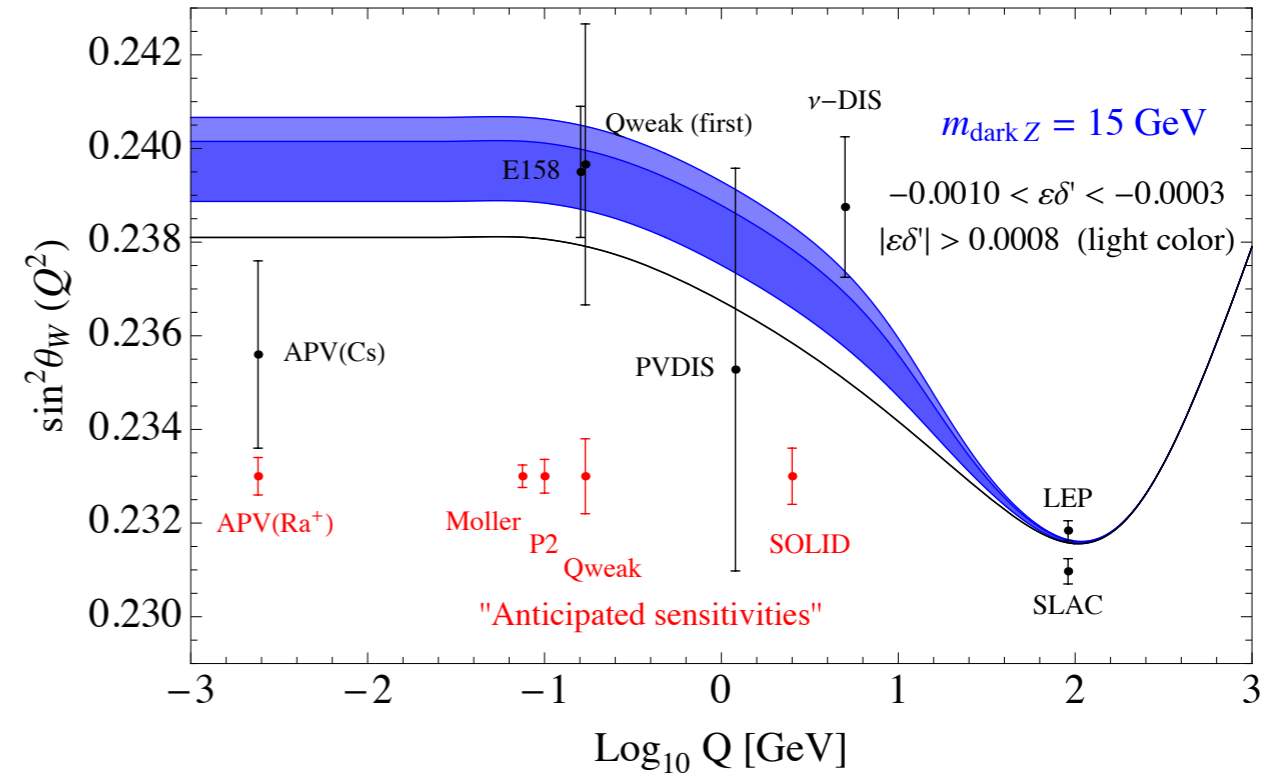
- Effective change in presence of dark-Z for parity violating asymmetries:

$$G_F \rightarrow \rho_d G_F$$

$$\sin^2 \theta_W \rightarrow \kappa_d \sin^2 \theta_W$$

$$\rho_d = 1 + \delta^2 \frac{m_{Z_d}^2}{Q^2 + m_{Z_d}^2}$$

$$\kappa_d = 1 - \frac{\varepsilon}{\varepsilon_Z} \delta^2 \frac{\cos \theta_W}{\sin \theta_W} \frac{m_{Z_d}^2}{Q^2 + m_{Z_d}^2}$$



EIC/ECCE Simulation Studies

[Boughazel, Emmert, Kutz, SM, Nycz, Petriello, Simsek, Wiegand, Zheng]

- Energy and integrated luminosity configurations used in the study:

Electron-Deuteron PVDIS		Electron-Proton PVDIS	
D1	5 GeV × 41 GeV eD , 4.4 fb ⁻¹	P1	5 GeV × 41 GeV ep , 4.4 fb ⁻¹
D2	5 GeV × 100 GeV eD , 36.8 fb ⁻¹	P2	5 GeV × 100 GeV ep , 36.8 fb ⁻¹
D3	10 GeV × 100 GeV eD , 44.8 fb ⁻¹	P3	10 GeV × 100 GeV ep , 44.8 fb ⁻¹
D4	10 GeV × 137 GeV eD , 100 fb ⁻¹	P4	10 GeV × 275 GeV ep , 100 fb ⁻¹
D5	18 GeV × 137 GeV eD , 15.4 fb ⁻¹	P5	18 GeV × 275 GeV ep , 15.4 fb ⁻¹
		P6	18 GeV × 275 GeV ep , 100 fb ⁻¹

- Also considered High Luminosity (HL) configurations corresponding to an increase by a factor of 10.
- 20 million MC events generated DJANGO + fast smearing method for each of the configurations above. 10 million events for $Q^2 > 1.0 \text{ GeV}^2$ and 10 million for $Q^2 > 50 \text{ GeV}^2$.
- Also, considered possibility of a positron beam.
- Observables studied:

$$A_{PV}^e, A_{PV}^p, A_{PV}^D, A_{LC}^p, A_{LC}^D$$

Asymmetry

Asymmetry Uncertainty

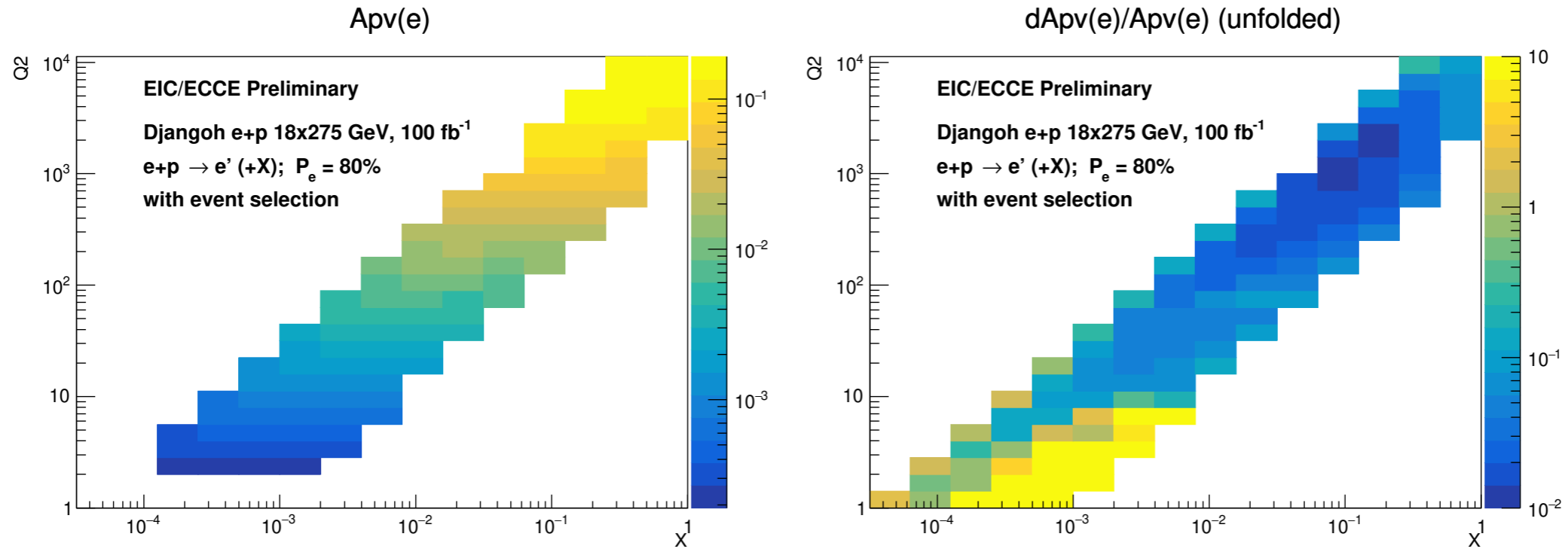


FIG. 3. Projection for $A_{PV}^{(e)}$ (left), and $dA_{PV,stat}^{(e)}/A_{PV}^{(e)}$ after unfolding (right) for 18×275 GeV ep collisions, with event-selection criteria applied. An integrated luminosity of 100 fb^{-1} and an electron polarization of 80% are assumed.

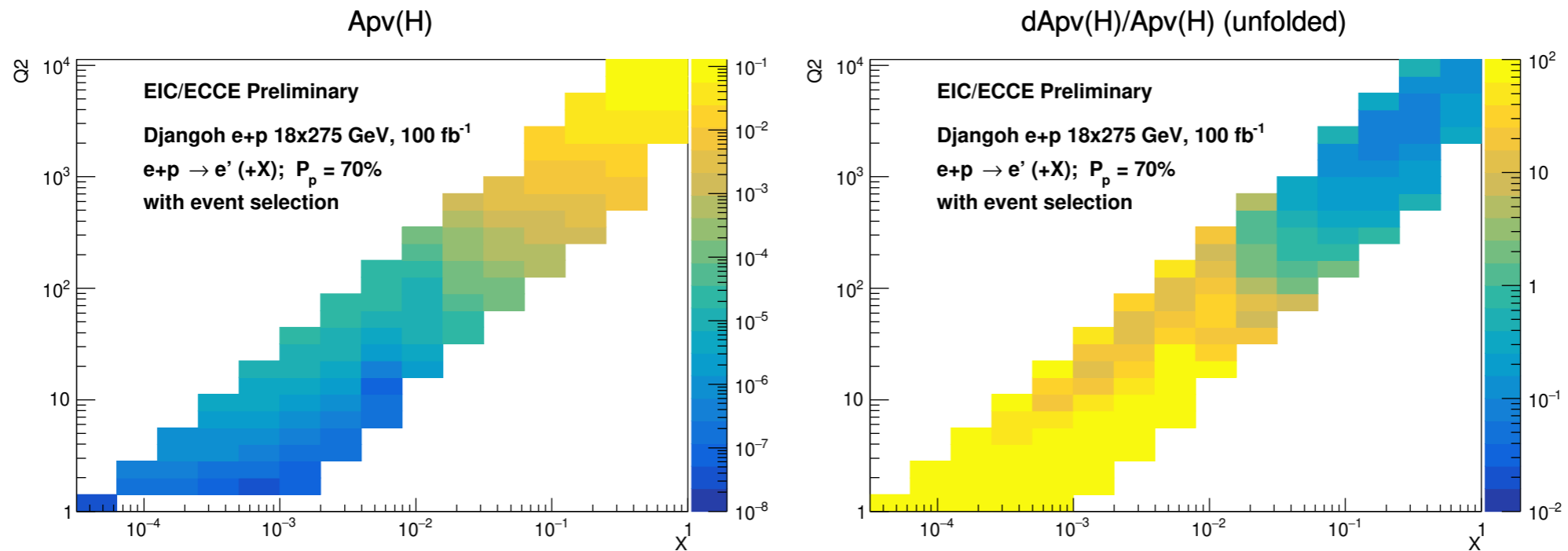
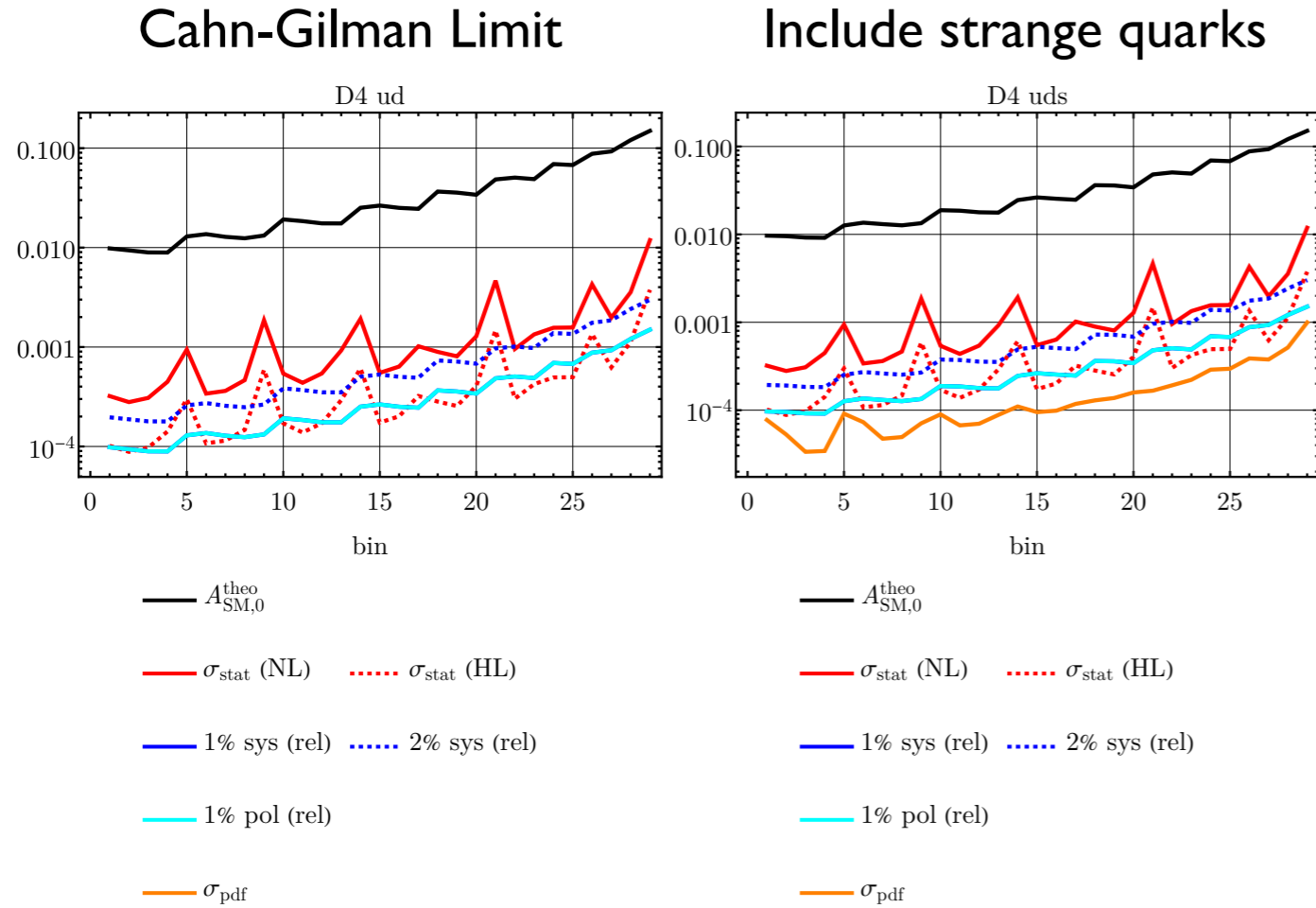


FIG. 4. Projection for $A_{PV}^{(p)}$ (left), and $dA_{PV,stat}^{(p)}/A_{PV}^{(p)}$ after unfolding (right) for 18×275 GeV ep collisions, with event-selection criteria applied. An integrated luminosity of 100 fb^{-1} and a proton polarization of 70% are assumed.

Electron-Deuteron PVDIS Asymmetry (A_{PV}^e)



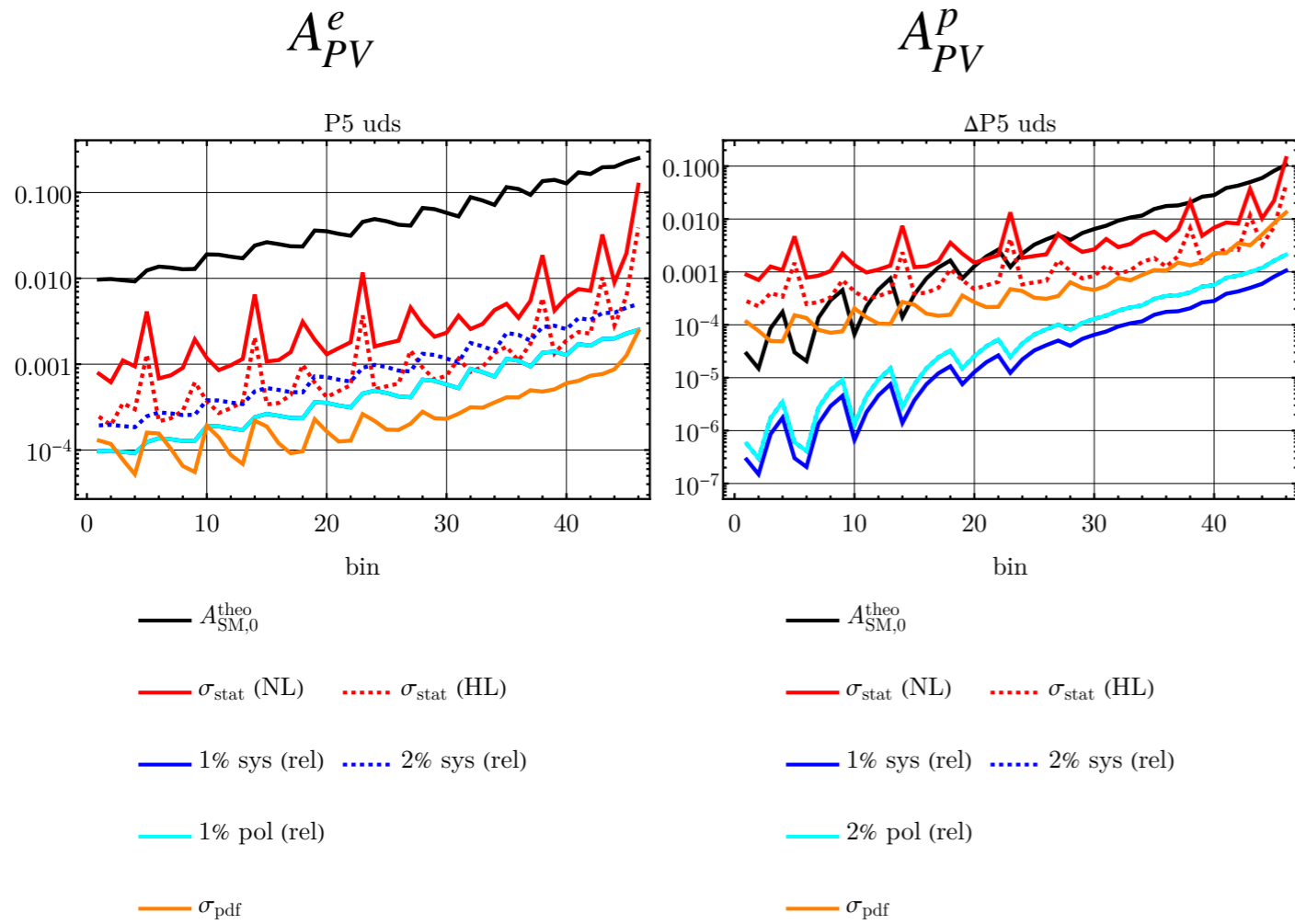
- Statistical uncertainty dominates
- PDF uncertainty has a small impact

FIG. 6. Comparison of the uncertainty components for the data set D4 in the valence-only scenario (ud) and with the contributions from the sea quarks (uds). Here, “NL” refers to the currently planned annual luminosity of the EIC, while “HL” refers to a potential ten-fold luminosity upgrade.

[Boughazel, Emmert, Kutz, SM, Nycz, Petriello, Simsek, Wiegand, Zheng]

D1	5 GeV × 41 GeV eD , 4.4 fb ⁻¹	P1	5 GeV × 41 GeV ep , 4.4 fb ⁻¹
D2	5 GeV × 100 GeV eD , 36.8 fb ⁻¹	P2	5 GeV × 100 GeV ep , 36.8 fb ⁻¹
D3	10 GeV × 100 GeV eD , 44.8 fb ⁻¹	P3	10 GeV × 100 GeV ep , 44.8 fb ⁻¹
D4	10 GeV × 137 GeV eD , 100 fb ⁻¹	P4	10 GeV × 275 GeV ep , 100 fb ⁻¹
D5	18 GeV × 137 GeV eD , 15.4 fb ⁻¹	P5	18 GeV × 275 GeV ep , 15.4 fb ⁻¹
		P6	18 GeV × 275 GeV ep , 100 fb ⁻¹

Electron-Proton PVDIS Asymmetries: A_{PV}^e and A_{PV}^p



- Statistical uncertainty dominates f
- PDF uncertainties have a small impact for A_{PV}^e but a significant impact for A_{PV}^p

[Boughazel, Emmert, Kutz, SM, Nycz, Petriello, Simsek, Wiegand, Zheng]

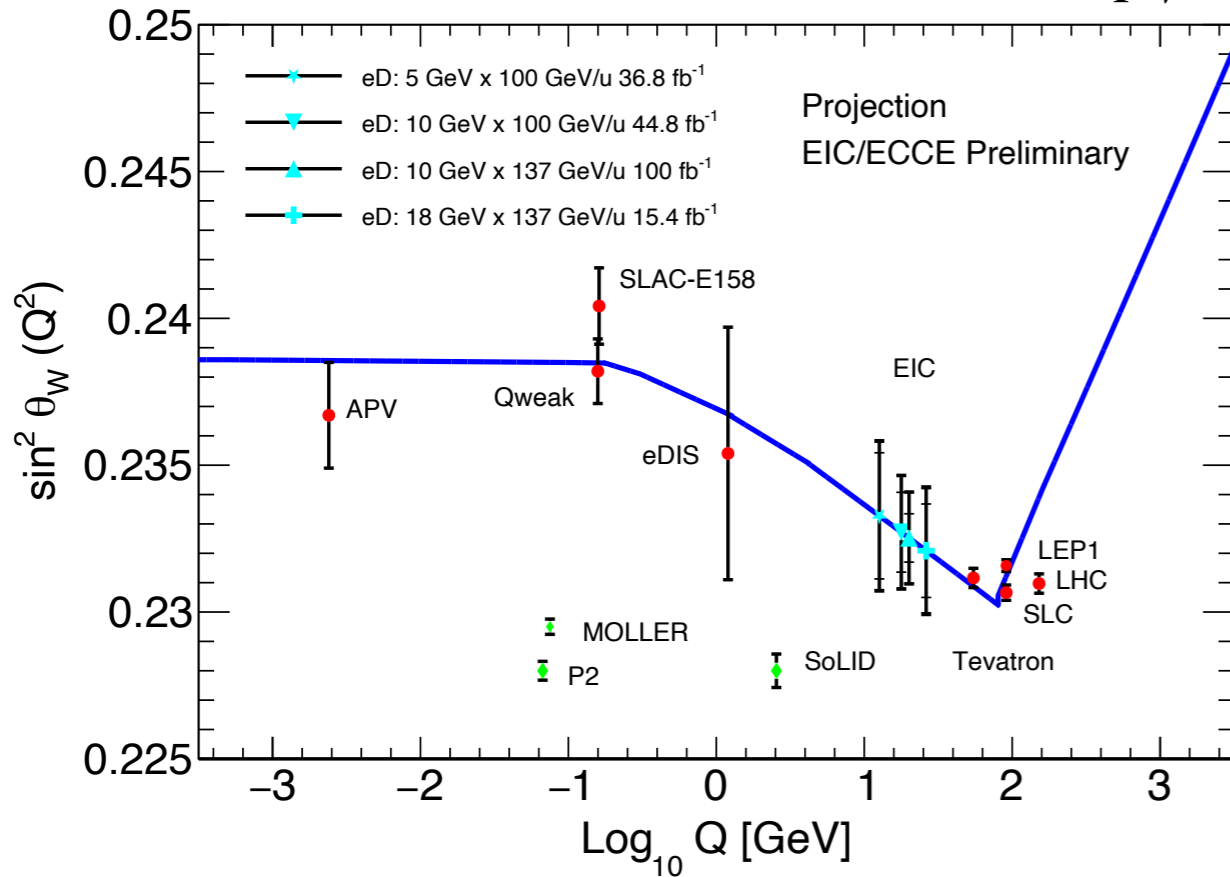
D1	5 GeV × 41 GeV eD , 4.4 fb ⁻¹	P1	5 GeV × 41 GeV ep , 4.4 fb ⁻¹
D2	5 GeV × 100 GeV eD , 36.8 fb ⁻¹	P2	5 GeV × 100 GeV ep , 36.8 fb ⁻¹
D3	10 GeV × 100 GeV eD , 44.8 fb ⁻¹	P3	10 GeV × 100 GeV ep , 44.8 fb ⁻¹
D4	10 GeV × 137 GeV eD , 100 fb ⁻¹	P4	10 GeV × 275 GeV ep , 100 fb ⁻¹
D5	18 GeV × 137 GeV eD , 15.4 fb ⁻¹	P5	18 GeV × 275 GeV ep , 15.4 fb ⁻¹
		P6	18 GeV × 275 GeV ep , 100 fb ⁻¹

Precision Extraction of the Weak Mixing Angle

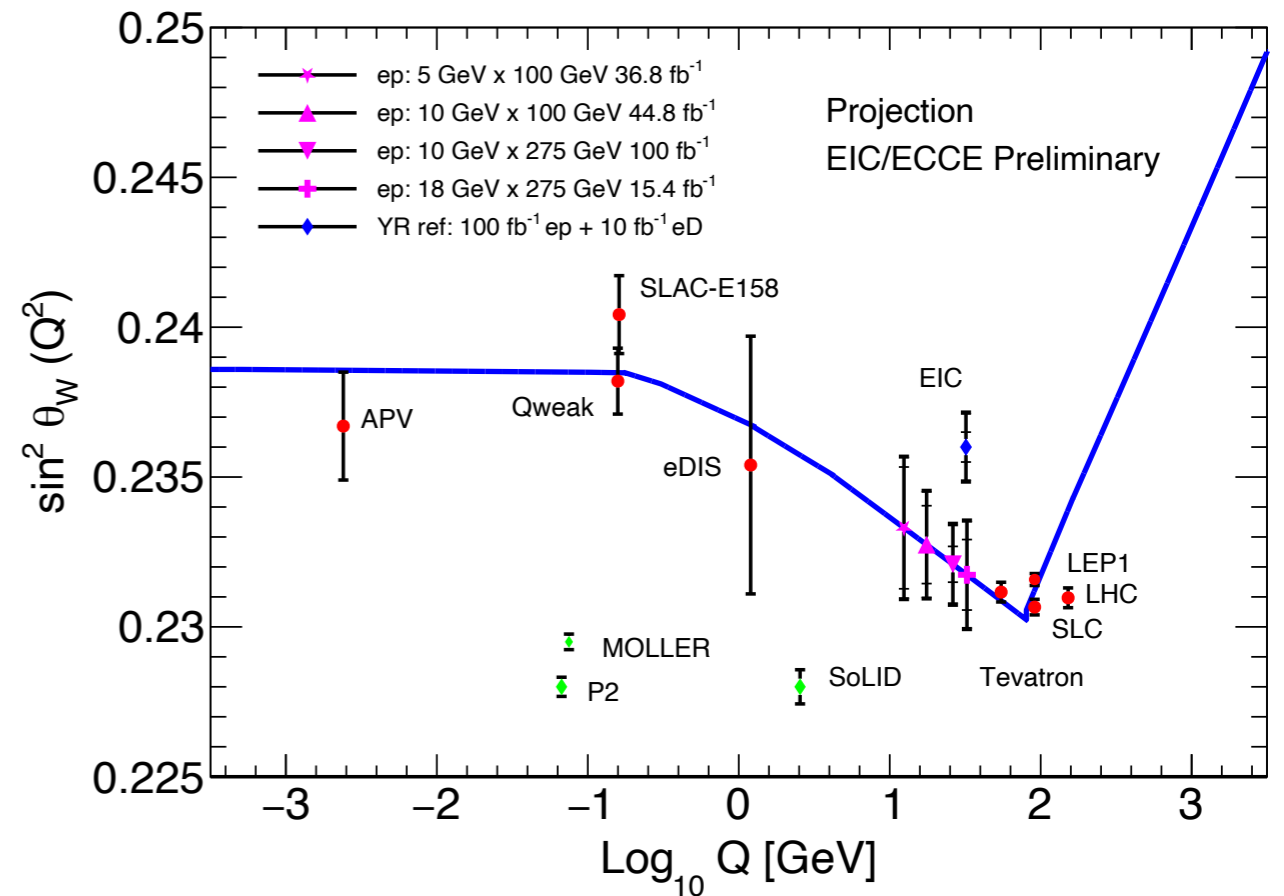
Projection for Extraction of the Weak Mixing Angle

[See talk by Nycz]

Electron-Deuteron PVDIS (A_{PV}^e)



Electron-Proton PVDIS (A_{PV}^e)



[Boughazel, Emmert, Kutz, SM, Nycz, Petriello, Simsek, Wiegand, Zheng]

- The EIC can extract the weak mixing angle over a previously unexplored range of Q^2
- Analysis included one loop \overline{MS} running including particle thresholds between Q^2 and M_Z

D1	5 GeV × 41 GeV <i>eD</i> , 4.4 fb ⁻¹	P1	5 GeV × 41 GeV <i>ep</i> , 4.4 fb ⁻¹
D2	5 GeV × 100 GeV <i>eD</i> , 36.8 fb ⁻¹	P2	5 GeV × 100 GeV <i>ep</i> , 36.8 fb ⁻¹
D3	10 GeV × 100 GeV <i>eD</i> , 44.8 fb ⁻¹	P3	10 GeV × 100 GeV <i>ep</i> , 44.8 fb ⁻¹
D4	10 GeV × 137 GeV <i>eD</i> , 100 fb ⁻¹	P4	10 GeV × 275 GeV <i>ep</i> , 100 fb ⁻¹
D5	18 GeV × 137 GeV <i>eD</i> , 15.4 fb ⁻¹	P5	18 GeV × 275 GeV <i>ep</i> , 15.4 fb ⁻¹
		P6	18 GeV × 275 GeV <i>ep</i> , 100 fb ⁻¹

- Projections for weak mixing angle extraction at the EIC from electron-proton PVDIS.

Beam type and energy Label	ep 5×100 P2	ep 10×100 P3	ep 10×275 P4	ep 18×275 P5	ep 18×275 P6
Luminosity (fb^{-1})	36.8	44.8	100	15.4	(100 YR ref)
$\langle Q^2 \rangle$ (GeV^2)	154.4	308.1	687.3	1055.1	1055.1
$\langle A_{PV} \rangle$ ($P_e = 0.8$)	-0.00854	-0.01617	-0.03254	-0.04594	-0.04594
$(dA/A)_{\text{stat}}$	1.54%	0.98%	0.40%	0.80%	(0.31%)
$(dA/A)_{\text{stat+syst(bg)}}$	1.55%	1.00%	0.43%	0.81%	(0.35%)
$(dA/A)_{1\% \text{pol}}$	1.0%	1.0%	1.0%	1.0%	(1.0%)
$(dA/A)_{\text{tot}}$	1.84%	1.42%	1.09%	1.29%	(1.06%)
Experimental					
$d(\sin^2 \theta_W)_{\text{stat+syst(bg)}}$	0.002032	0.001299	0.000597	0.001176	0.000516
$d(\sin^2 \theta_W)_{\text{stat+syst+pol}}$	0.002342	0.001759	0.001297	0.001769	0.001244
with PDF					
$d(\sin^2 \theta_W)_{\text{tot,CT18NLO}}$	0.002388	0.001807	0.001363	0.001823	0.001320
$d(\sin^2 \theta_W)_{\text{tot,MMHT2014}}$	0.002353	0.001771	0.001319	0.001781	0.001270
$d(\sin^2 \theta_W)_{\text{tot,NNPDF31}}$	0.002351	0.001789	0.001313	0.001801	0.001308

TABLE III. Projected PVDIS asymmetry and fitted results for $\sin^2 \theta_W$ using ep collision data and the nominal annual luminosity. Here, $\langle Q^2 \rangle$ denotes the value averaged over all (x, Q^2) bins, weighted by $(dA/A)_{\text{stat}}^{-2}$ for each bin. The electron beam polarization is assumed to be 80% with a relative 1% uncertainty. The total (“tot”) uncertainty is from combining all of statistical, 1% systematic (background), 1% beam polarization, and PDF uncertainties evaluated using three different PDF sets. The rightmost column is for comparison with the YR.

- Projections for weak mixing angle extraction at the EIC from electron-deuteron PVDIS.

Beam type and energy Label	eD 5×100 D2	eD 10×100 D3	eD 10×137 D4	eD 18×137 D5	eD 18×137 N/A
Luminosity (fb^{-1})	36.8	44.8	100	15.4	(10 YR ref)
$\langle Q^2 \rangle$ (GeV^2)	160.0	316.9	403.5	687.2	687.2
$\langle A_{PV} \rangle$ ($P_e = 0.8$)	-0.01028	-0.01923	-0.02366	-0.03719	-0.03719
$(dA/A)_{\text{stat}}$	1.46%	0.93%	0.54%	1.05%	(1.31%)
$(dA/A)_{\text{stat+bg}}$	1.47%	0.95%	0.56%	1.07%	(1.32%)
$(dA/A)_{\text{syst,1\%pol}}$	1.0%	1.0%	1.0%	1.0%	(1.0%)
$(dA/A)_{\text{tot}}$	1.78%	1.38%	1.15%	1.46%	(1.66%)
Experimental					
$d(\sin^2 \theta_W)_{\text{stat+bg}}$	0.002148	0.001359	0.000823	0.001591	0.001963
$d(\sin^2 \theta_W)_{\text{stat+bg+pol}}$	0.002515	0.001904	0.001544	0.002116	0.002414
with PDF					
$d(\sin^2 \theta_W)_{\text{tot,CT18}}$	0.002558	0.001936	0.001566	0.002173	0.00247
$d(\sin^2 \theta_W)_{\text{tot,MMHT2014}}$	0.002527	0.001917	0.001562	0.002128	0.002424
$d(\sin^2 \theta_W)_{\text{tot,NNPDF31}}$	0.002526	0.001915	0.001560	0.002127	0.002423

TABLE IV. Projected PVDIS asymmetry and fitted results for $\sin^2 \theta_W$ using eD collision data and the nominal annual luminosity. The uncertainty evaluation is the same as Table III.

SMEFT Analysis

Standard Model Effective Theory (SMEFT)

Operator Basis

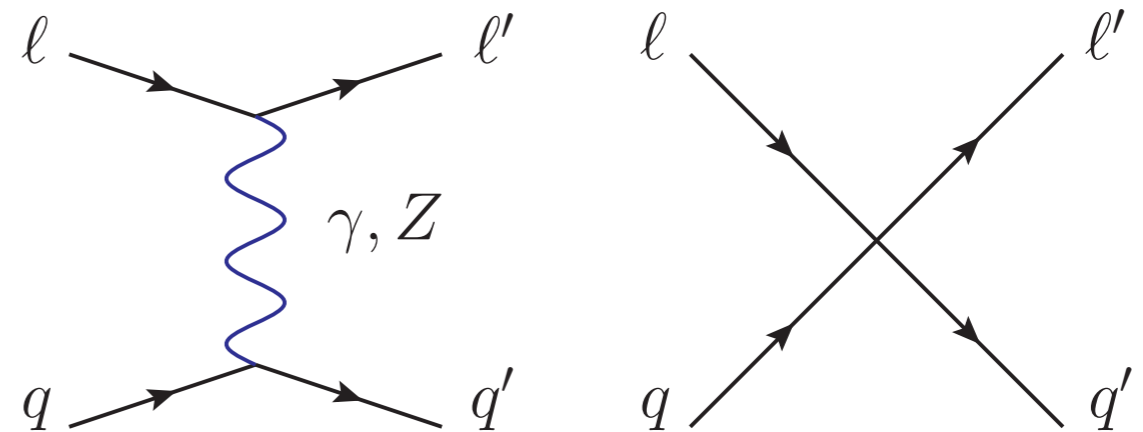
[Boughazel, Petriello, Wiegand]

- The SMEFT basis often used in global fit analysis to constrain new physics beyond the electroweak scale:

$$\mathcal{L} = \mathcal{L}_{SM} + \frac{1}{\Lambda^2} \sum_i C_i^6 \mathcal{O}_{6,i} + \frac{1}{\Lambda^4} \sum_i C_i^8 \mathcal{O}_{8,i} + \dots$$

- Relevant SMEFT operators for DIS processes at dim-6 and dim-8

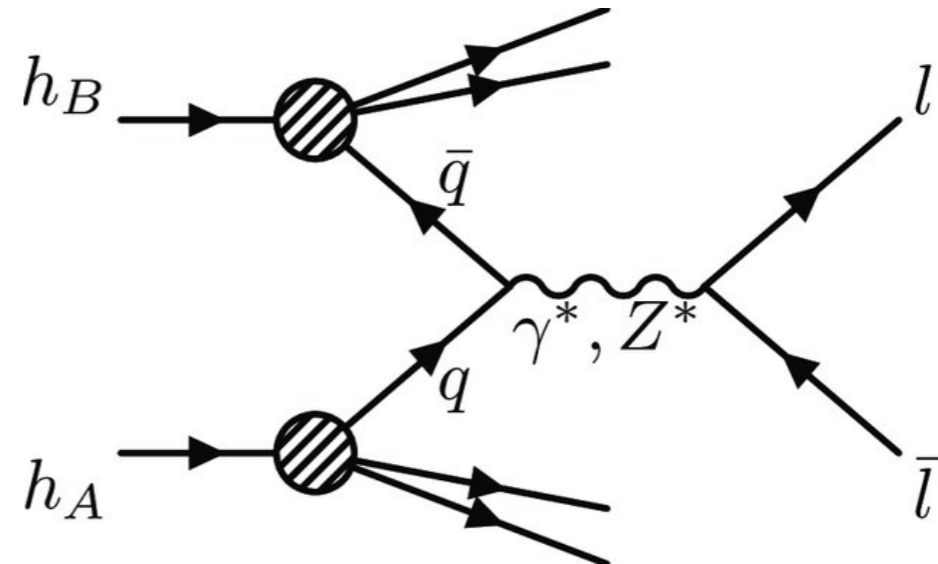
Dimension 6		Dimension 8	
$\mathcal{O}_{lq}^{(1)}$	$(\bar{l}\gamma^\mu l)(\bar{q}\gamma_\mu q)$	$\mathcal{O}_{l^2 q^2 D^2}^{(1)}$	$D^\nu (\bar{l}\gamma^\mu l) D_\nu (\bar{q}\gamma_\mu q)$
$\mathcal{O}_{lq}^{(3)}$	$(\bar{l}\gamma^\mu \tau^i l)(\bar{q}\gamma_\mu \tau^i q)$	$\mathcal{O}_{l^2 q^2 D^2}^{(3)}$	$D^\nu (\bar{l}\gamma^\mu \tau^i l) D_\nu (\bar{q}\gamma_\mu \tau^i q)$
\mathcal{O}_{eu}	$(\bar{e}\gamma^\mu e)(\bar{u}\gamma_\mu u)$	$\mathcal{O}_{e^2 u^2 D^2}^{(1)}$	$D^\nu (\bar{e}\gamma^\mu e) D_\nu (\bar{u}\gamma_\mu u)$
\mathcal{O}_{ed}	$(\bar{e}\gamma^\mu e)(\bar{d}\gamma_\mu d)$	$\mathcal{O}_{e^2 d^2 D^2}^{(1)}$	$D^\nu (\bar{e}\gamma^\mu e) D_\nu (\bar{d}\gamma_\mu d)$
\mathcal{O}_{lu}	$(\bar{l}\gamma^\mu l)(\bar{u}\gamma_\mu u)$	$\mathcal{O}_{l^2 u^2 D^2}^{(1)}$	$D^\nu (\bar{l}\gamma^\mu l) D_\nu (\bar{u}\gamma_\mu u)$
\mathcal{O}_{ld}	$(\bar{l}\gamma^\mu l)(\bar{d}\gamma_\mu d)$	$\mathcal{O}_{l^2 d^2 D^2}^{(1)}$	$D^\nu (\bar{l}\gamma^\mu l) D_\nu (\bar{d}\gamma_\mu d)$
\mathcal{O}_{qe}	$(\bar{q}\gamma^\mu q)(\bar{e}\gamma_\mu e)$	$\mathcal{O}_{q^2 e^2 D^2}^{(1)}$	$D^\nu (\bar{q}\gamma^\mu q) D_\nu (\bar{e}\gamma_\mu e)$



SMEFT Constraints from Drell-Yan at LHC

[Boughazel, Petriello, Wiegand]

- The SMEFT Wilson coefficients that affect PVES also contribute to the Drell-Yan process at the LHC

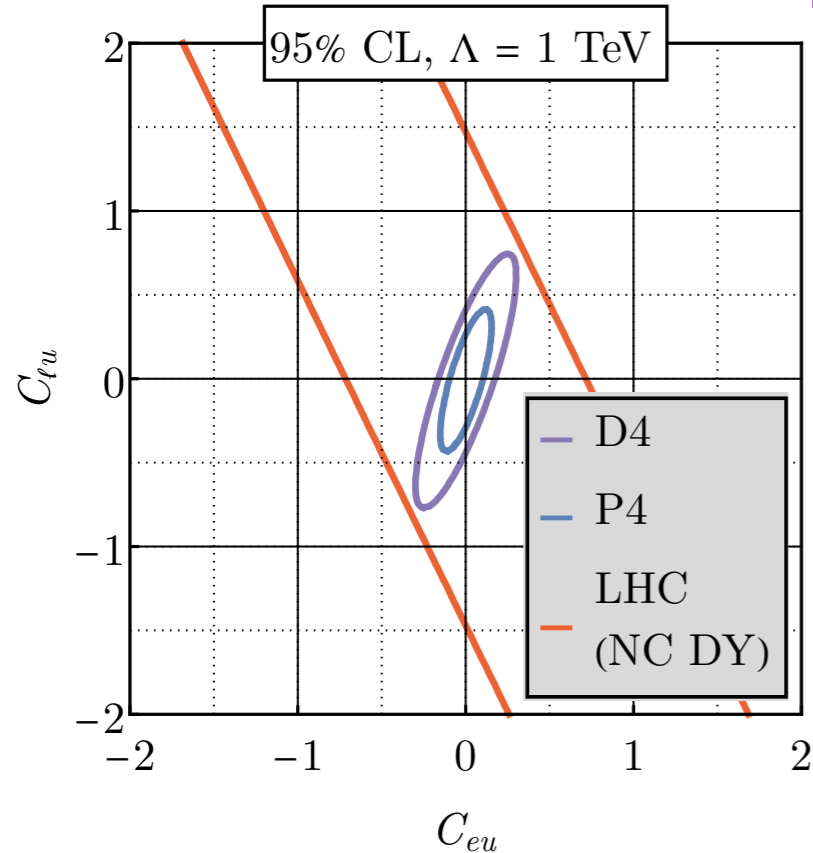


$$\frac{d\sigma_{q\bar{q}}}{dm_{ll}^2 dY dc_\theta} = \frac{1}{32\pi m_{ll}^2 \hat{s}} f_q(x_1) f_{\bar{q}}(x_2) \left\{ \frac{d\hat{\sigma}_{q\bar{q}}^{\gamma\gamma}}{dm_{ll}^2 dY dc_\theta} + \frac{d\hat{\sigma}_{q\bar{q}}^{\gamma Z}}{dm_{ll}^2 dY dc_\theta} + \frac{d\hat{\sigma}_{q\bar{q}}^{ZZ}}{dm_{ll}^2 dY dc_\theta} \right. \\ \left. + \frac{d\hat{\sigma}_{q\bar{q}}^{\gamma SMEFT6}}{dm_{ll}^2 dY dc_\theta} + \frac{d\hat{\sigma}_{q\bar{q}}^{Z SMEFT6}}{dm_{ll}^2 dY dc_\theta} + \frac{d\hat{\sigma}_{q\bar{q}}^{\gamma SMEFT8}}{dm_{ll}^2 dY dc_\theta} + \frac{d\hat{\sigma}_{q\bar{q}}^{Z SMEFT8}}{dm_{ll}^2 dY dc_\theta} + \frac{d\hat{\sigma}_{q\bar{q}}^{SMEFT6^2}}{dm_{ll}^2 dY dc_\theta} \right\}$$

- PVES and the LHC can be complementary to each other in constraining new physics

Constraining BSM and Lifting Flat Directions

[Boughazel, Emmert, Kutz, SM, Nycz, Petriello, Simsek, Wiegand, Zheng]



- PVDIS and Drell-Yan at the LHC are sensitive to different combinations of the SMEFT Wilson coefficients.

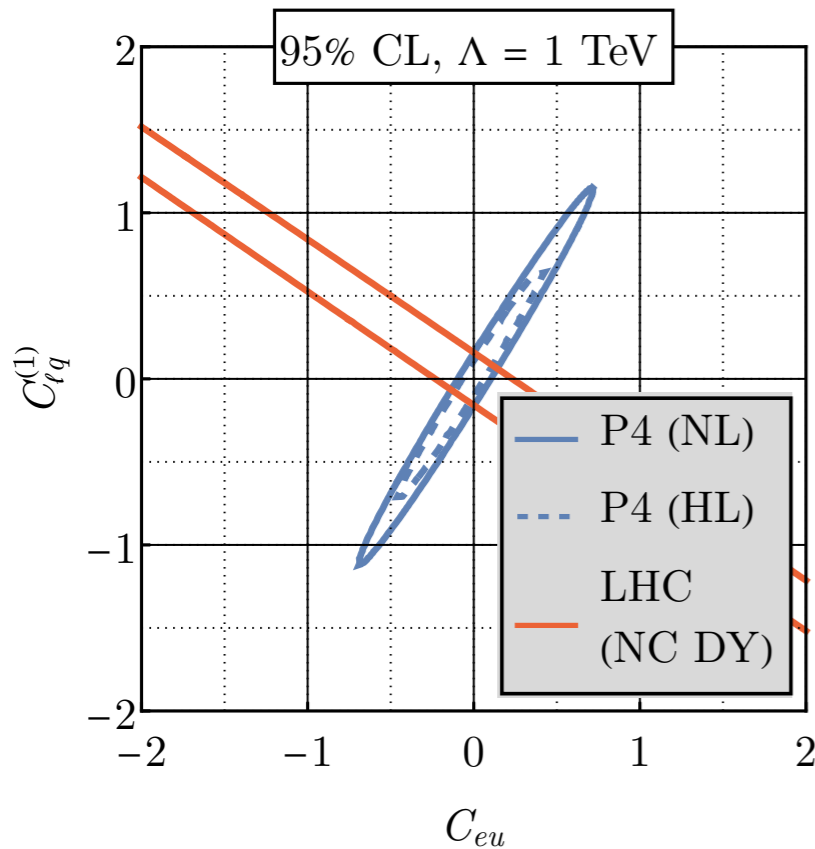
- PVDIS can lift “flat directions” by probing orthogonal directions in the SMEFT parameter space compared to the LHC

Dimension 6		Dimension 8	
$\mathcal{O}_{lq}^{(1)}$	$(\bar{l}\gamma^\mu l)(\bar{q}\gamma_\mu q)$	$\mathcal{O}_{l^2q^2D^2}^{(1)}$	$D^\nu(\bar{l}\gamma^\mu l)D_\nu(\bar{q}\gamma_\mu q)$
$\mathcal{O}_{lq}^{(3)}$	$(\bar{l}\gamma^\mu\tau^i l)(\bar{q}\gamma_\mu\tau^i q)$	$\mathcal{O}_{l^2q^2D^2}^{(3)}$	$D^\nu(\bar{l}\gamma^\mu\tau^i l)D_\nu(\bar{q}\gamma_\mu\tau^i q)$
\mathcal{O}_{eu}	$(\bar{e}\gamma^\mu e)(\bar{u}\gamma_\mu u)$	$\mathcal{O}_{e^2u^2D^2}^{(1)}$	$D^\nu(\bar{e}\gamma^\mu e)D_\nu(\bar{u}\gamma_\mu u)$
\mathcal{O}_{ed}	$(\bar{e}\gamma^\mu e)(\bar{d}\gamma_\mu d)$	$\mathcal{O}_{e^2d^2D^2}^{(1)}$	$D^\nu(\bar{e}\gamma^\mu e)D_\nu(\bar{d}\gamma_\mu d)$
\mathcal{O}_{lu}	$(\bar{l}\gamma^\mu l)(\bar{u}\gamma_\mu u)$	$\mathcal{O}_{l^2u^2D^2}^{(1)}$	$D^\nu(\bar{l}\gamma^\mu l)D_\nu(\bar{u}\gamma_\mu u)$
\mathcal{O}_{ld}	$(\bar{l}\gamma^\mu l)(\bar{d}\gamma_\mu d)$	$\mathcal{O}_{l^2d^2D^2}^{(1)}$	$D^\nu(\bar{l}\gamma^\mu l)D_\nu(\bar{d}\gamma_\mu d)$
\mathcal{O}_{qe}	$(\bar{q}\gamma^\mu q)(\bar{e}\gamma_\mu e)$	$\mathcal{O}_{q^2e^2D^2}^{(1)}$	$D^\nu(\bar{q}\gamma^\mu q)D_\nu(\bar{e}\gamma_\mu e)$

D1	5 GeV × 41 GeV eD , 4.4 fb ⁻¹	P1	5 GeV × 41 GeV ep , 4.4 fb ⁻¹
D2	5 GeV × 100 GeV eD , 36.8 fb ⁻¹	P2	5 GeV × 100 GeV ep , 36.8 fb ⁻¹
D3	10 GeV × 100 GeV eD , 44.8 fb ⁻¹	P3	10 GeV × 100 GeV ep , 44.8 fb ⁻¹
D4	10 GeV × 137 GeV eD , 100 fb ⁻¹	P4	10 GeV × 275 GeV ep , 100 fb ⁻¹
D5	18 GeV × 137 GeV eD , 15.4 fb ⁻¹	P5	18 GeV × 275 GeV ep , 15.4 fb ⁻¹
		P6	18 GeV × 275 GeV ep , 100 fb ⁻¹

Constraining BSM and Lifting Flat Directions

[Boughazel, Emmert, Kutz, SM, Nycz, Petriello, Simsek, Wiegand, Zheng]



- PVDIS and Drell-Yan at the LHC are sensitive to different combinations of the SMEFT Wilson coefficients.

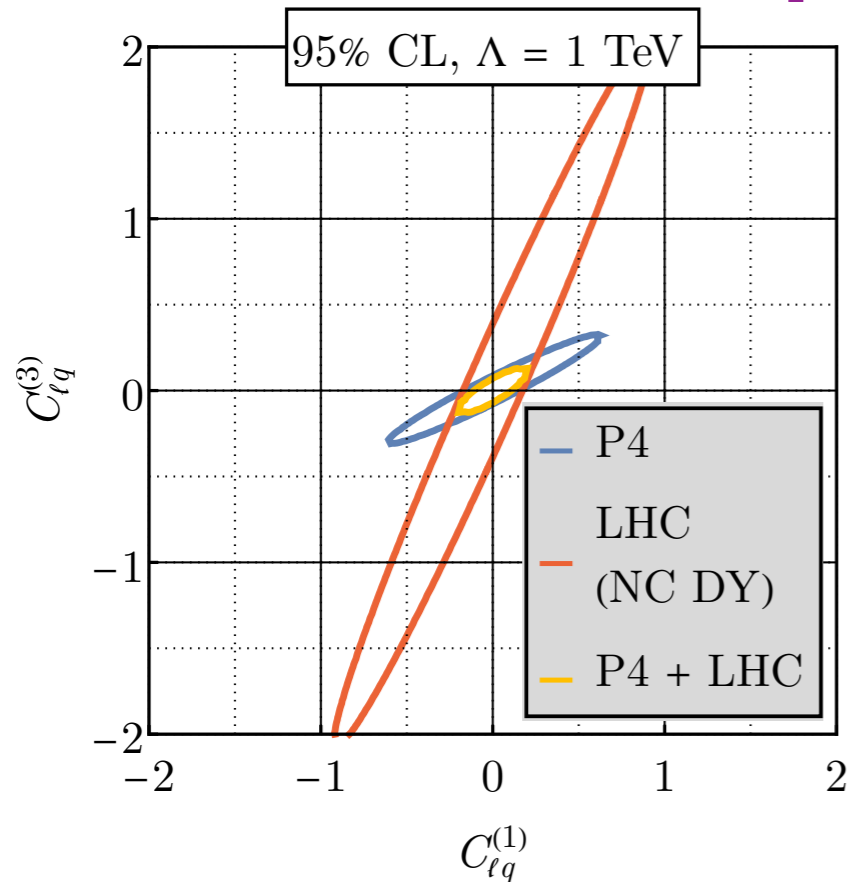
- PVDIS can lift “flat directions” by probing orthogonal directions in the SMEFT parameter space compared to the LHC

Dimension 6		Dimension 8	
$\mathcal{O}_{lq}^{(1)}$	$(\bar{l}\gamma^\mu l)(\bar{q}\gamma_\mu q)$	$\mathcal{O}_{l^2 q^2 D^2}^{(1)}$	$D^\nu (\bar{l}\gamma^\mu l) D_\nu (\bar{q}\gamma_\mu q)$
$\mathcal{O}_{lq}^{(3)}$	$(\bar{l}\gamma^\mu \tau^i l)(\bar{q}\gamma_\mu \tau^i q)$	$\mathcal{O}_{l^2 q^2 D^2}^{(3)}$	$D^\nu (\bar{l}\gamma^\mu \tau^i l) D_\nu (\bar{q}\gamma_\mu \tau^i q)$
\mathcal{O}_{eu}	$(\bar{e}\gamma^\mu e)(\bar{u}\gamma_\mu u)$	$\mathcal{O}_{e^2 u^2 D^2}^{(1)}$	$D^\nu (\bar{e}\gamma^\mu e) D_\nu (\bar{u}\gamma_\mu u)$
\mathcal{O}_{ed}	$(\bar{e}\gamma^\mu e)(\bar{d}\gamma_\mu d)$	$\mathcal{O}_{e^2 d^2 D^2}^{(1)}$	$D^\nu (\bar{e}\gamma^\mu e) D_\nu (\bar{d}\gamma_\mu d)$
\mathcal{O}_{lu}	$(\bar{l}\gamma^\mu l)(\bar{u}\gamma_\mu u)$	$\mathcal{O}_{l^2 u^2 D^2}^{(1)}$	$D^\nu (\bar{l}\gamma^\mu l) D_\nu (\bar{u}\gamma_\mu u)$
\mathcal{O}_{ld}	$(\bar{l}\gamma^\mu l)(\bar{d}\gamma_\mu d)$	$\mathcal{O}_{l^2 d^2 D^2}^{(1)}$	$D^\nu (\bar{l}\gamma^\mu l) D_\nu (\bar{d}\gamma_\mu d)$
\mathcal{O}_{qe}	$(\bar{q}\gamma^\mu q)(\bar{e}\gamma_\mu e)$	$\mathcal{O}_{q^2 e^2 D^2}^{(1)}$	$D^\nu (\bar{q}\gamma^\mu q) D_\nu (\bar{e}\gamma_\mu e)$

D1	5 GeV × 41 GeV eD , 4.4 fb ⁻¹	P1	5 GeV × 41 GeV ep , 4.4 fb ⁻¹
D2	5 GeV × 100 GeV eD , 36.8 fb ⁻¹	P2	5 GeV × 100 GeV ep , 36.8 fb ⁻¹
D3	10 GeV × 100 GeV eD , 44.8 fb ⁻¹	P3	10 GeV × 100 GeV ep , 44.8 fb ⁻¹
D4	10 GeV × 137 GeV eD , 100 fb ⁻¹	P4	10 GeV × 275 GeV ep , 100 fb ⁻¹
D5	18 GeV × 137 GeV eD , 15.4 fb ⁻¹	P5	18 GeV × 275 GeV ep , 15.4 fb ⁻¹
		P6	18 GeV × 275 GeV ep , 100 fb ⁻¹

Constraining BSM and Lifting Flat Directions

[Boughazel, Emmert, Kutz, SM, Nycz, Petriello, Simsek, Wiegand, Zheng]



- PVDIS and Drell-Yan at the LHC are sensitive to different combinations of the SMEFT Wilson coefficients.

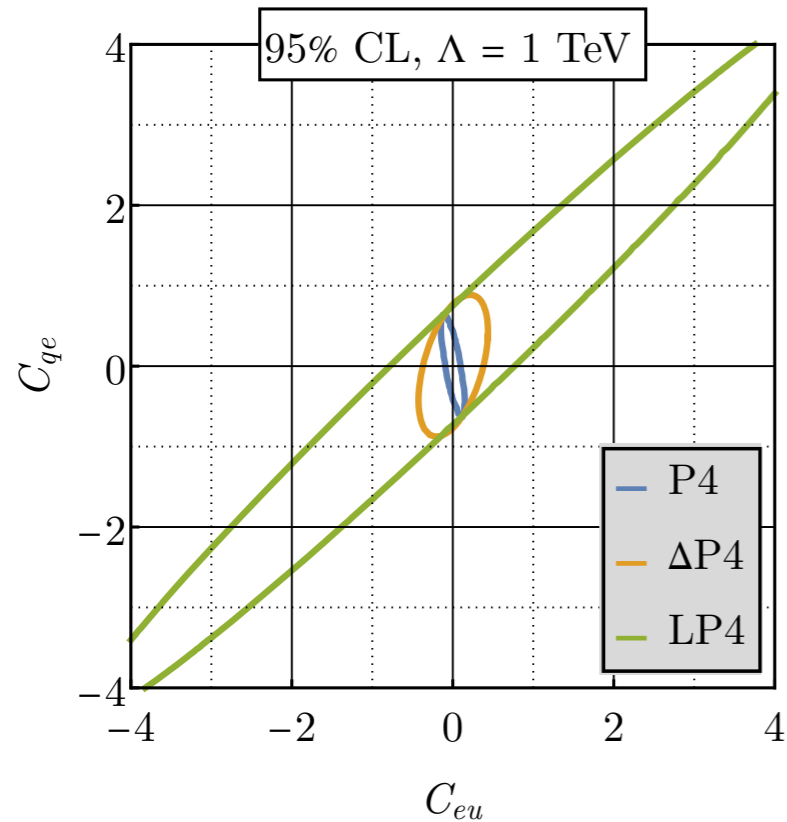
- PVDIS can lift “flat directions” by probing orthogonal directions in the SMEFT parameter space compared to the LHC

Dimension 6		Dimension 8	
$\mathcal{O}_{lq}^{(1)}$	$(\bar{l}\gamma^\mu l)(\bar{q}\gamma_\mu q)$	$\mathcal{O}_{l^2 q^2 D^2}^{(1)}$	$D^\nu (\bar{l}\gamma^\mu l) D_\nu (\bar{q}\gamma_\mu q)$
$\mathcal{O}_{lq}^{(3)}$	$(\bar{l}\gamma^\mu \tau^i l)(\bar{q}\gamma_\mu \tau^i q)$	$\mathcal{O}_{l^2 q^2 D^2}^{(3)}$	$D^\nu (\bar{l}\gamma^\mu \tau^i l) D_\nu (\bar{q}\gamma_\mu \tau^i q)$
\mathcal{O}_{eu}	$(\bar{e}\gamma^\mu e)(\bar{u}\gamma_\mu u)$	$\mathcal{O}_{e^2 u^2 D^2}^{(1)}$	$D^\nu (\bar{e}\gamma^\mu e) D_\nu (\bar{u}\gamma_\mu u)$
\mathcal{O}_{ed}	$(\bar{e}\gamma^\mu e)(\bar{d}\gamma_\mu d)$	$\mathcal{O}_{e^2 d^2 D^2}^{(1)}$	$D^\nu (\bar{e}\gamma^\mu e) D_\nu (\bar{d}\gamma_\mu d)$
\mathcal{O}_{lu}	$(\bar{l}\gamma^\mu l)(\bar{u}\gamma_\mu u)$	$\mathcal{O}_{l^2 u^2 D^2}^{(1)}$	$D^\nu (\bar{l}\gamma^\mu l) D_\nu (\bar{u}\gamma_\mu u)$
\mathcal{O}_{ld}	$(\bar{l}\gamma^\mu l)(\bar{d}\gamma_\mu d)$	$\mathcal{O}_{l^2 d^2 D^2}^{(1)}$	$D^\nu (\bar{l}\gamma^\mu l) D_\nu (\bar{d}\gamma_\mu d)$
\mathcal{O}_{qe}	$(\bar{q}\gamma^\mu q)(\bar{e}\gamma_\mu e)$	$\mathcal{O}_{q^2 e^2 D^2}^{(1)}$	$D^\nu (\bar{q}\gamma^\mu q) D_\nu (\bar{e}\gamma_\mu e)$

D1	5 GeV × 41 GeV eD , 4.4 fb ⁻¹	P1	5 GeV × 41 GeV ep , 4.4 fb ⁻¹
D2	5 GeV × 100 GeV eD , 36.8 fb ⁻¹	P2	5 GeV × 100 GeV ep , 36.8 fb ⁻¹
D3	10 GeV × 100 GeV eD , 44.8 fb ⁻¹	P3	10 GeV × 100 GeV ep , 44.8 fb ⁻¹
D4	10 GeV × 137 GeV eD , 100 fb ⁻¹	P4	10 GeV × 275 GeV ep , 100 fb ⁻¹
D5	18 GeV × 137 GeV eD , 15.4 fb ⁻¹	P5	18 GeV × 275 GeV ep , 15.4 fb ⁻¹
		P6	18 GeV × 275 GeV ep , 100 fb ⁻¹

Constraining BSM and Lifting Flat Directions

[Boughazel, Emmert, Kutz, SM, Nycz, Petriello, Simsek, Wiegand, Zheng]



- PVDIS and Drell-Yan at the LHC are sensitive to different combinations of the SMEFT Wilson coefficients.

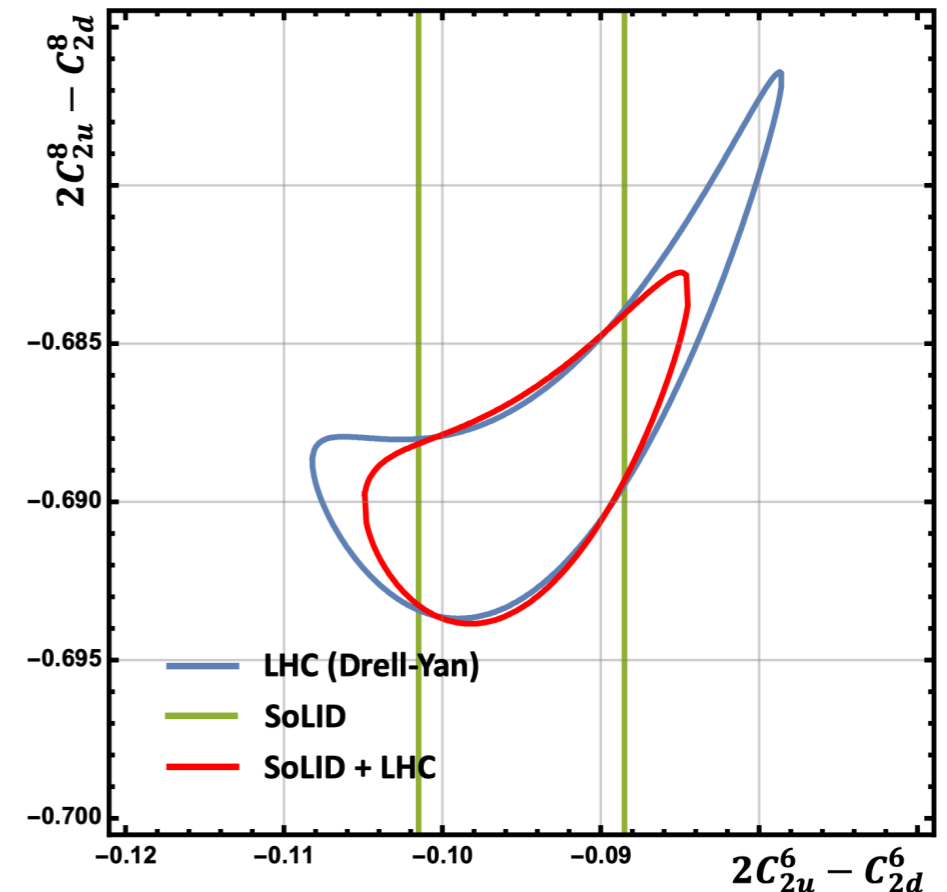
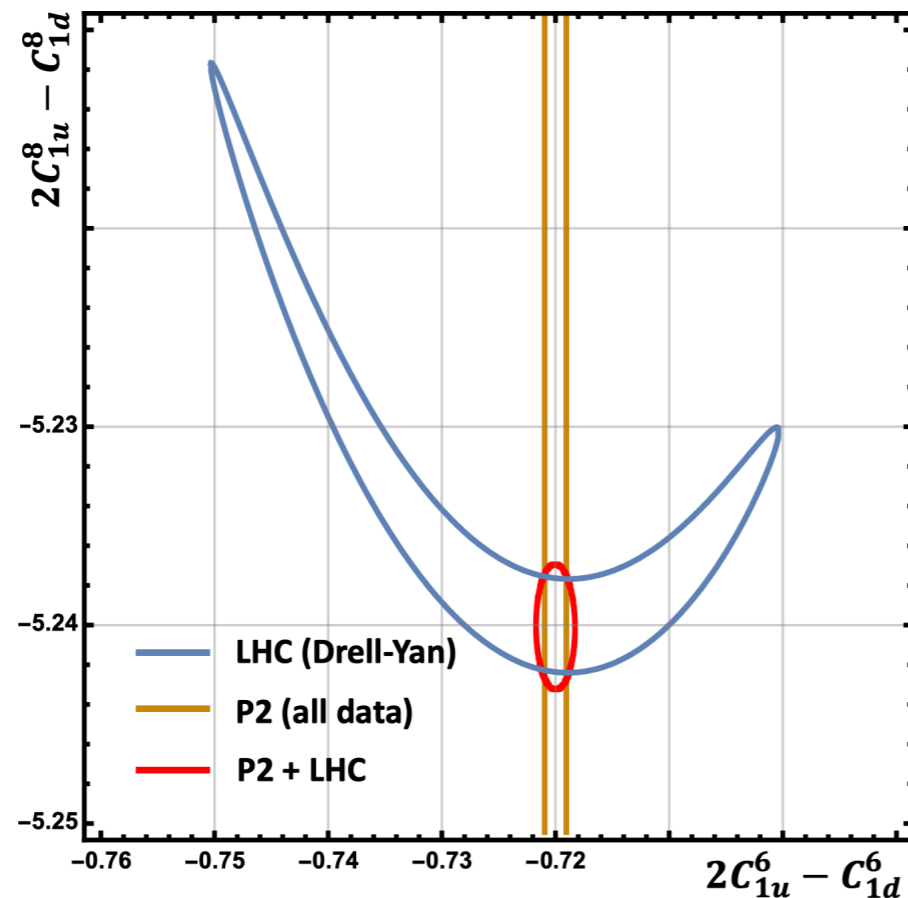
- PVDIS can lift “flat directions” by probing orthogonal directions in the SMEFT parameter space compared to the LHC

Dimension 6		Dimension 8	
$\mathcal{O}_{lq}^{(1)}$	$(\bar{l}\gamma^\mu l)(\bar{q}\gamma_\mu q)$	$\mathcal{O}_{l^2 q^2 D^2}^{(1)}$	$D^\nu (\bar{l}\gamma^\mu l) D_\nu (\bar{q}\gamma_\mu q)$
$\mathcal{O}_{lq}^{(3)}$	$(\bar{l}\gamma^\mu \tau^i l)(\bar{q}\gamma_\mu \tau^i q)$	$\mathcal{O}_{l^2 q^2 D^2}^{(3)}$	$D^\nu (\bar{l}\gamma^\mu \tau^i l) D_\nu (\bar{q}\gamma_\mu \tau^i q)$
\mathcal{O}_{eu}	$(\bar{e}\gamma^\mu e)(\bar{u}\gamma_\mu u)$	$\mathcal{O}_{e^2 u^2 D^2}^{(1)}$	$D^\nu (\bar{e}\gamma^\mu e) D_\nu (\bar{u}\gamma_\mu u)$
\mathcal{O}_{ed}	$(\bar{e}\gamma^\mu e)(\bar{d}\gamma_\mu d)$	$\mathcal{O}_{e^2 d^2 D^2}^{(1)}$	$D^\nu (\bar{e}\gamma^\mu e) D_\nu (\bar{d}\gamma_\mu d)$
\mathcal{O}_{lu}	$(\bar{l}\gamma^\mu l)(\bar{u}\gamma_\mu u)$	$\mathcal{O}_{l^2 u^2 D^2}^{(1)}$	$D^\nu (\bar{l}\gamma^\mu l) D_\nu (\bar{u}\gamma_\mu u)$
\mathcal{O}_{ld}	$(\bar{l}\gamma^\mu l)(\bar{d}\gamma_\mu d)$	$\mathcal{O}_{l^2 d^2 D^2}^{(1)}$	$D^\nu (\bar{l}\gamma^\mu l) D_\nu (\bar{d}\gamma_\mu d)$
\mathcal{O}_{qe}	$(\bar{q}\gamma^\mu q)(\bar{e}\gamma_\mu e)$	$\mathcal{O}_{q^2 e^2 D^2}^{(1)}$	$D^\nu (\bar{q}\gamma^\mu q) D_\nu (\bar{e}\gamma_\mu e)$

D1	5 GeV \times 41 GeV eD , 4.4 fb $^{-1}$	P1	5 GeV \times 41 GeV ep , 4.4 fb $^{-1}$
D2	5 GeV \times 100 GeV eD , 36.8 fb $^{-1}$	P2	5 GeV \times 100 GeV ep , 36.8 fb $^{-1}$
D3	10 GeV \times 100 GeV eD , 44.8 fb $^{-1}$	P3	10 GeV \times 100 GeV ep , 44.8 fb $^{-1}$
D4	10 GeV \times 137 GeV eD , 100 fb $^{-1}$	P4	10 GeV \times 275 GeV ep , 100 fb $^{-1}$
D5	18 GeV \times 137 GeV eD , 15.4 fb $^{-1}$	P5	18 GeV \times 275 GeV ep , 15.4 fb $^{-1}$
		P6	18 GeV \times 275 GeV ep , 100 fb $^{-1}$

Disentangling Dim-6 and Dim-8 SMEFT Operators

[Boughazel, Petriello, Wiegand]



- Another advantage of low energy PVES experiments:

The large energy of the LHC can make it difficult to disentangle the effects of dim-6 or dim-8 (and dim-6 squared) operators.

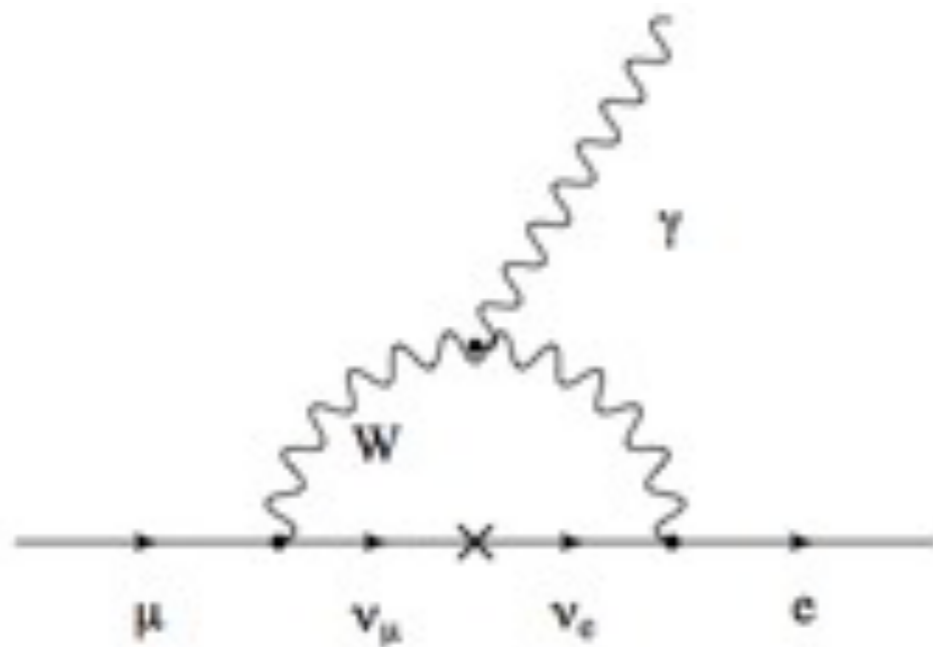
Low energy PVES will only have sensitivity to dim-6 operators providing valuable input to disentangle dim-6 vs dim-8.

This is also true at the EIC

Charged Lepton Flavor Violation

Lepton Flavor Violation

- Discovery of neutrino oscillations indicate that neutrinos have mass!
- Neutrino oscillations imply Lepton Flavor Violation (LFV).
- LFV in the neutrinos also implies Charged Lepton Flavor Violation (CLFV):



$$\text{BR}(\mu \rightarrow e\gamma) < 10^{-54}$$

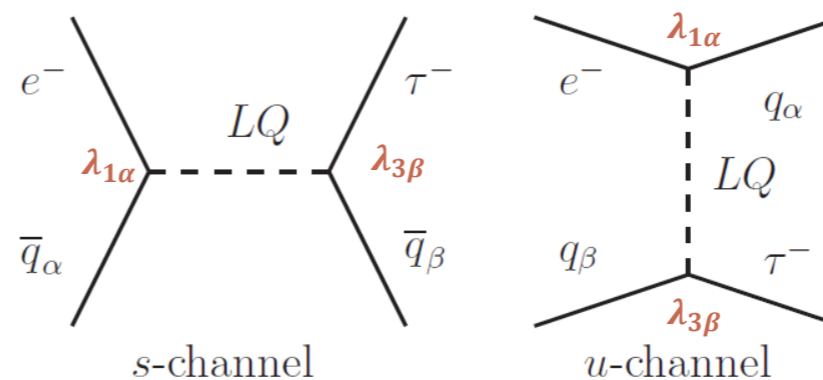
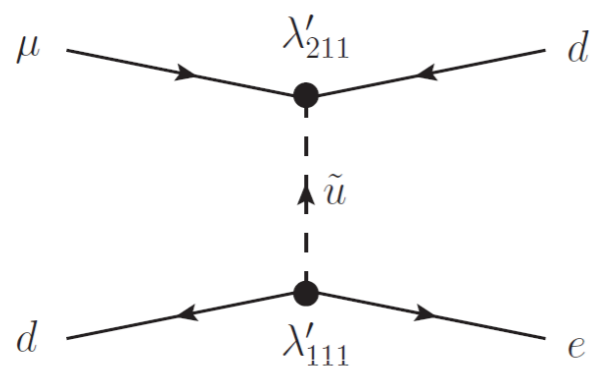
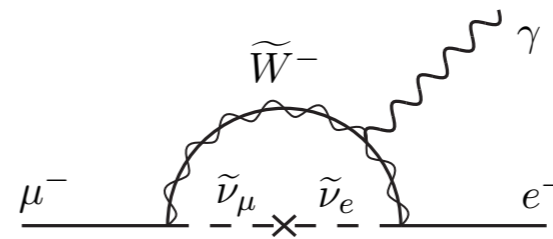
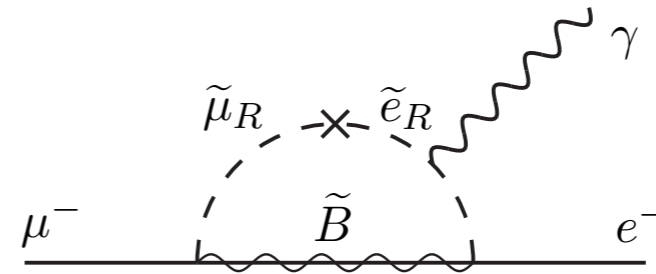
However, SM rate for CLFV is tiny due to small neutrino masses

- No hope of detecting such small rates for CLFV at any present or future planned experiments!

Lepton Flavor Violation in BSM

- However, many BSM scenarios predict enhanced CLFV rates:

- SUSY (RPV)
- SU(5), SO(10) GUTS
- Left-Right symmetric models
- Randall-Sundrum Models
- LeptoQuarks
- ...



- Leptoquarks can generate CLFV at tree level! Likely to produce enhanced CLFV rates compared to loop level processes in other models.

Charged Lepton Flavor Violation Limits

- Present and future limits:

Process	Experiment	Limit (90% <i>C. L.</i>)	Year
$\mu \rightarrow e\gamma$	MEGA	$Br < 1.2 \times 10^{-11}$	2002
$\mu + Au \rightarrow e + Au$	SINDRUM II	$\Gamma_{conv}/\Gamma_{capt} < 7.0 \times 10^{-13}$	2006
$\mu \rightarrow 3e$	SINDRUM	$Br < 1.0 \times 10^{-12}$	1988
$\tau \rightarrow e\gamma$	BaBar	$Br < 3.3 \times 10^{-8}$	2010
$\tau \rightarrow \mu\gamma$	BaBar	$Br < 6.8 \times 10^{-8}$	2005
$\tau \rightarrow 3e$	BELLE	$Br < 3.6 \times 10^{-8}$	2008
$\mu + N \rightarrow e + N$	Mu2e	$\Gamma_{conv}/\Gamma_{capt} < 6.0 \times 10^{-17}$	2017?
$\mu \rightarrow e\gamma$	MEG	$Br \lesssim 10^{-13}$	2011?
$\tau \rightarrow e\gamma$	Super-B	$Br \lesssim 10^{-10}$	> 2020?

- Note that CLFV(1,2) is severely constrained. Limits on CLFV(1,3) are weaker by several orders of magnitude.
- Limits on CLFV(1,2) are expected to improve even further in future experiments.

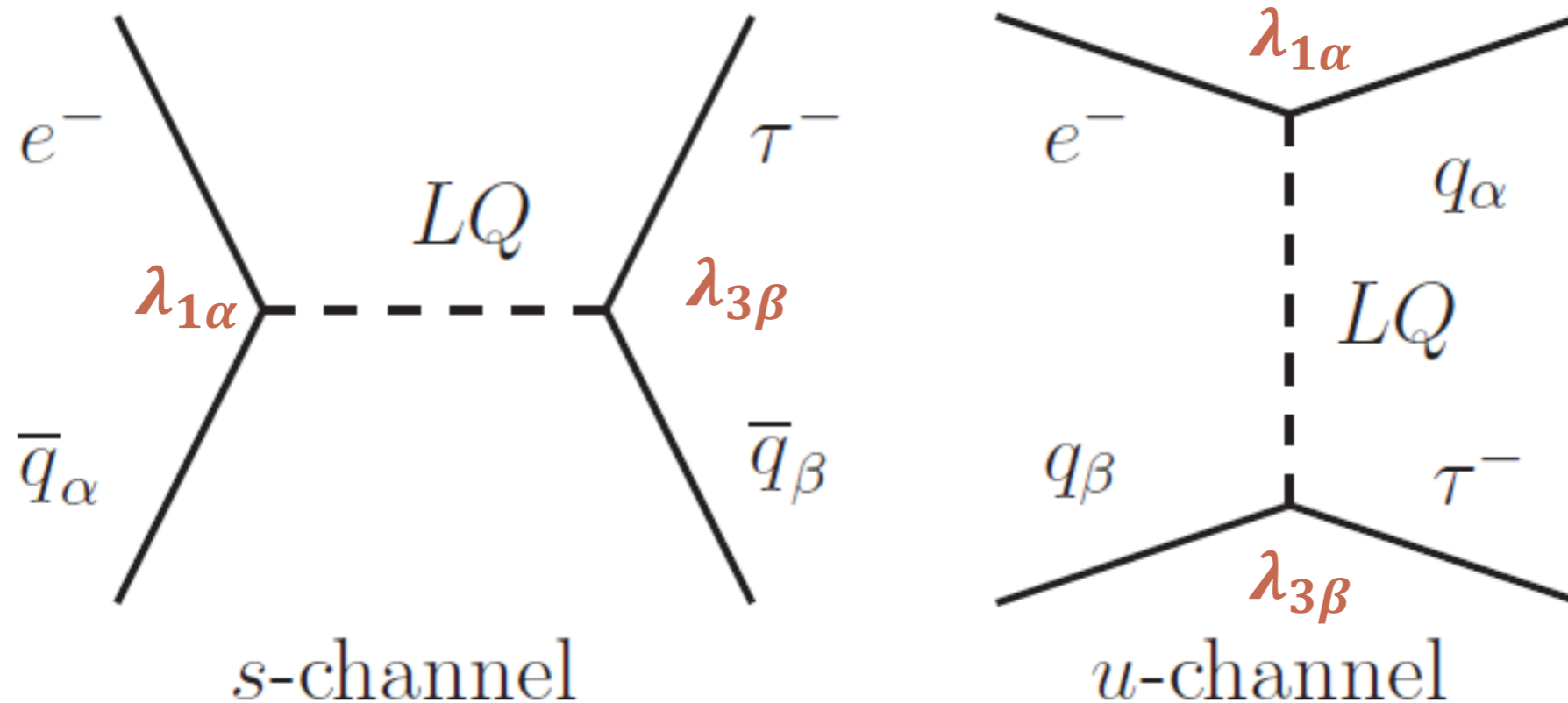
CLFV in DIS

[M.Gonderinger, M.Ramsey-Musolf]
[Cirigliano, Fuyuto, Lee, Mereghetti, Yan]

- The EIC can search for CLFV(1,3) in the DIS process:

$$ep \rightarrow \tau X$$

- Such a process could be mediated, for example, by leptoquarks:



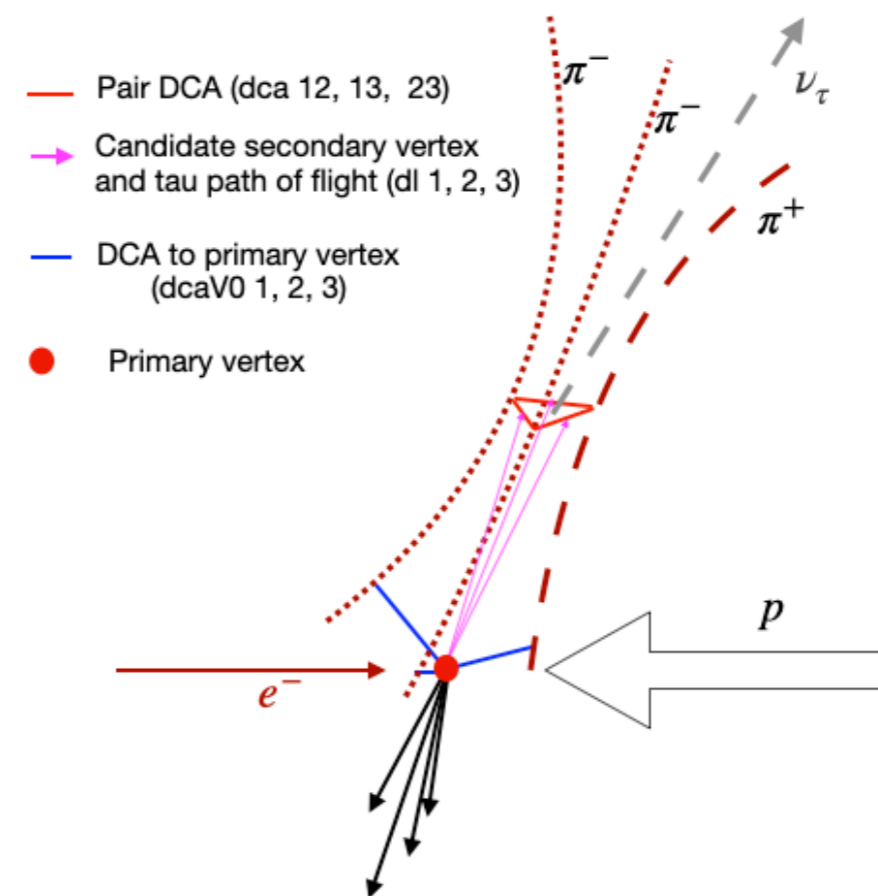
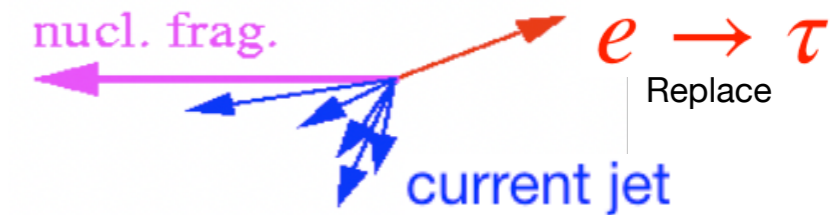
- CLFV can also be studied in the SMEFT framework

[See talk by Mereghetti]

CLFV simulation

- CLFV at EIC: search for $e+p \rightarrow \tau+X$ events
- Key task: tau identification
- First focus on 3-prong decay:
 - primary vertex and missing energy reconstruction
 - **secondary vertex reconstruction with vertex tracker**
- Event generators:
 - LQGENEP 1.0 for Leptoquark events (L. Bellagamba, 2001)
 - DJANGO 4.6.8 for DIS (NC + CC) events (H. Spiesberger 2005)
- Jets reconstructed from MC events
 - Fastjet, Anti- k_T , $R = 1.0$
 - Scattered electron for SM DIS and neutrinos excluded
- Detector simulation
 - Fun4All + ECCE configurations with different magnetic fields

[EIC/ECCE Collaboration]



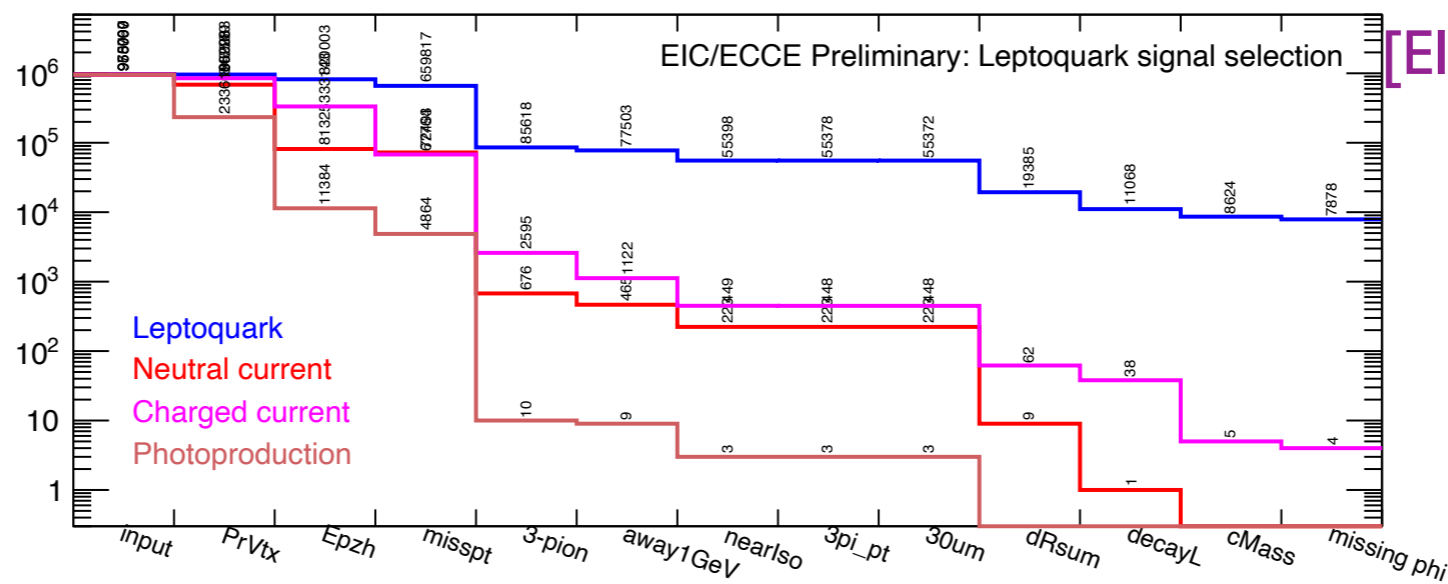


Figure 4: MC statistics of leptoquark (blue), DIS CC (red), DIS NC (magenta), and photoproduction (orange) events, as ten selection criteria are progressively applied on 1 M input events for each channel. Please see text for details.

D1	5 GeV × 41 GeV eD , 4.4 fb ⁻¹	P1	5 GeV × 41 GeV ep , 4.4 fb ⁻¹
D2	5 GeV × 100 GeV eD , 36.8 fb ⁻¹	P2	5 GeV × 100 GeV ep , 36.8 fb ⁻¹
D3	10 GeV × 100 GeV eD , 44.8 fb ⁻¹	P3	10 GeV × 100 GeV ep , 44.8 fb ⁻¹
D4	10 GeV × 137 GeV eD , 100 fb ⁻¹	P4	10 GeV × 275 GeV ep , 100 fb ⁻¹
D5	18 GeV × 137 GeV eD , 15.4 fb ⁻¹	P5	18 GeV × 275 GeV ep , 15.4 fb ⁻¹
		P6	18 GeV × 275 GeV ep , 100 fb ⁻¹

- Simulated 1M events for each of the signal and background processes
- For 100fb⁻¹ this corresponds to particular cross section sizes for the signal and background events.
- The number of selected events in each background channel is then scaled to the true cross section value.
- The number of selected signal events is scaled to the required number that satisfies:

$$S / \sqrt{(B)} \geq 5$$

- This scaled number of signal events corresponds to a signal cross section at 100fb⁻¹ which corresponds to the needed EIC signal cross section sensitivity.

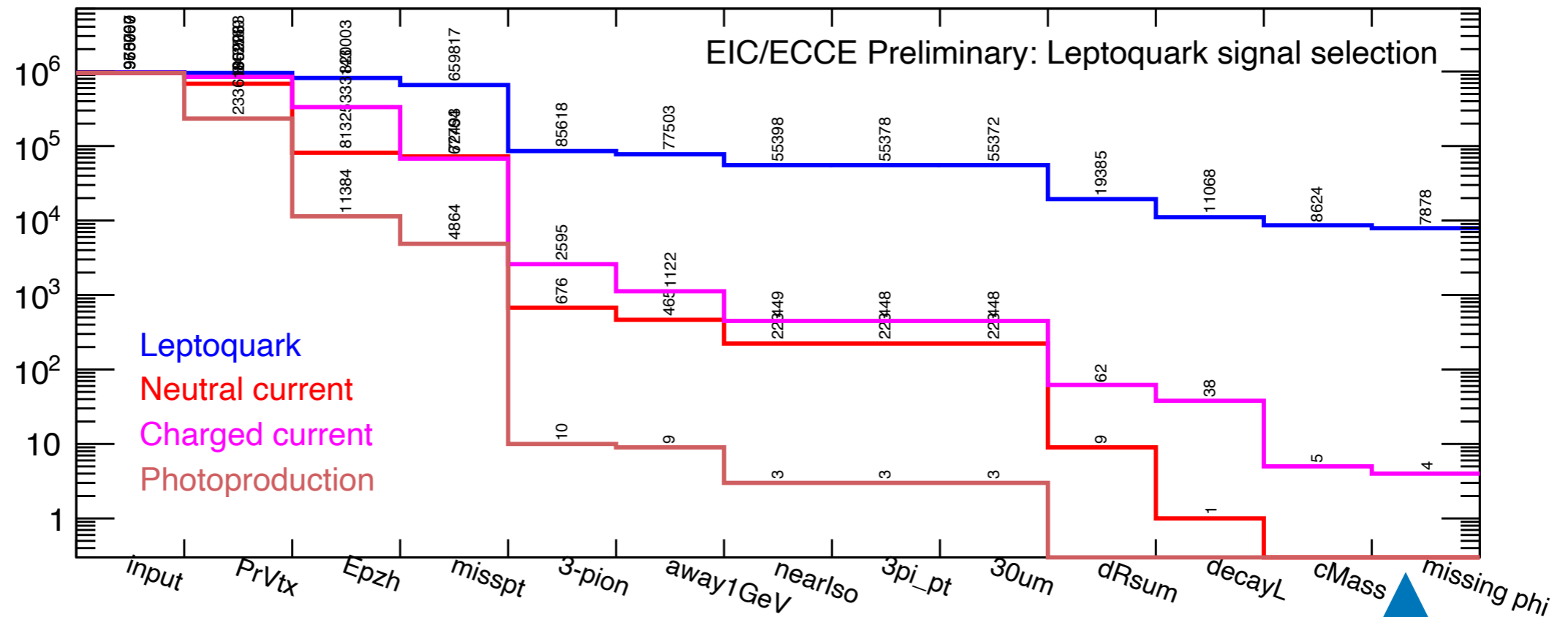


Figure 4: MC statistics of leptoquark (blue), DIS CC (red), DIS NC (magenta), and photoproduction (orange) events, as ten selection criteria are progressively applied on 1 M input events for each channel. Please see text for details.

Zero background events survive for NC DIS and Photoproduction

Need 1B simulation events to match the true cross sections for NC DIS + photoproduction to see how many background events survive.

[See talk by Buni]

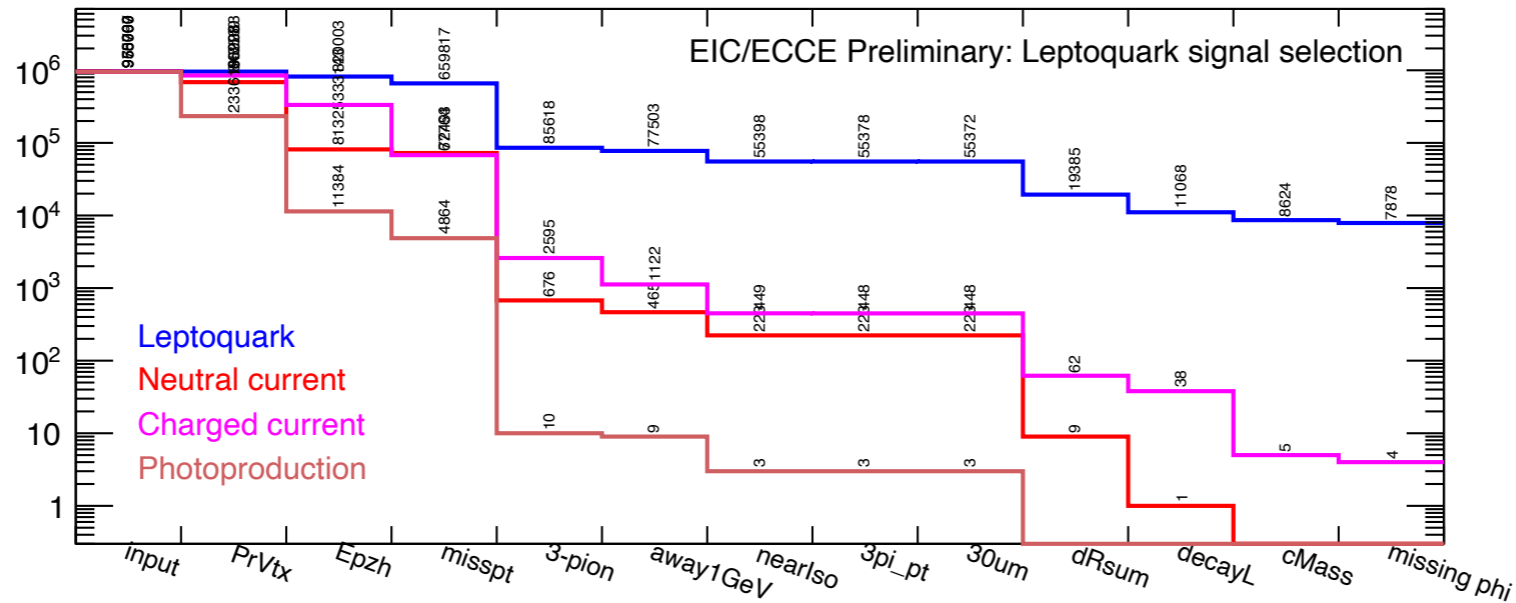
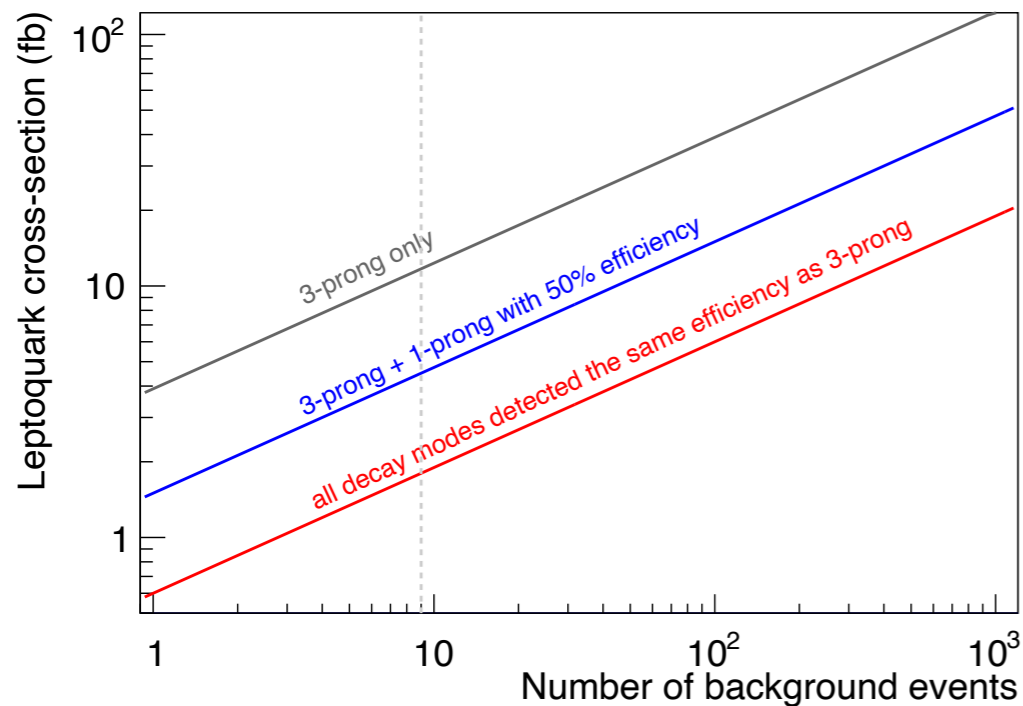


Figure 4: MC statistics of leptoquark (blue), DIS CC (red), DIS NC (magenta), and photoproduction (orange) events, as ten selection criteria are progressively applied on 1 M input events for each channel. Please see text for details.



EIC sensitivity to signal cross section as a function of the number of background events that survive.

$$S / \sqrt{B} \geq 5$$

Figure 6: Cross section sensitivity for leptoquark search vs number of residual background events for 100 fb^{-1} integrated luminosity. The grey line corresponds to the scenario that only “3-prong” decay modes are detected. The blue line corresponds to the scenario where electron and pion “1-prong” decay modes could be detected with 50% efficiency of the “3-prong” case. And the red line shows the scenario if all decay modes were detected at the same efficiency as the “3-prong” case.

$$\sigma_{F=0} = \sum_{\alpha,\beta} \frac{s}{32\pi} \left[\frac{\lambda_{1\alpha}\lambda_{3\beta}}{M_{LQ}^2} \right]^2 \left\{ \int dx dy x \bar{q}_\alpha(x, xs) f(y) + \int dx dy x q_\beta(x, -u) g(y) \right\}$$

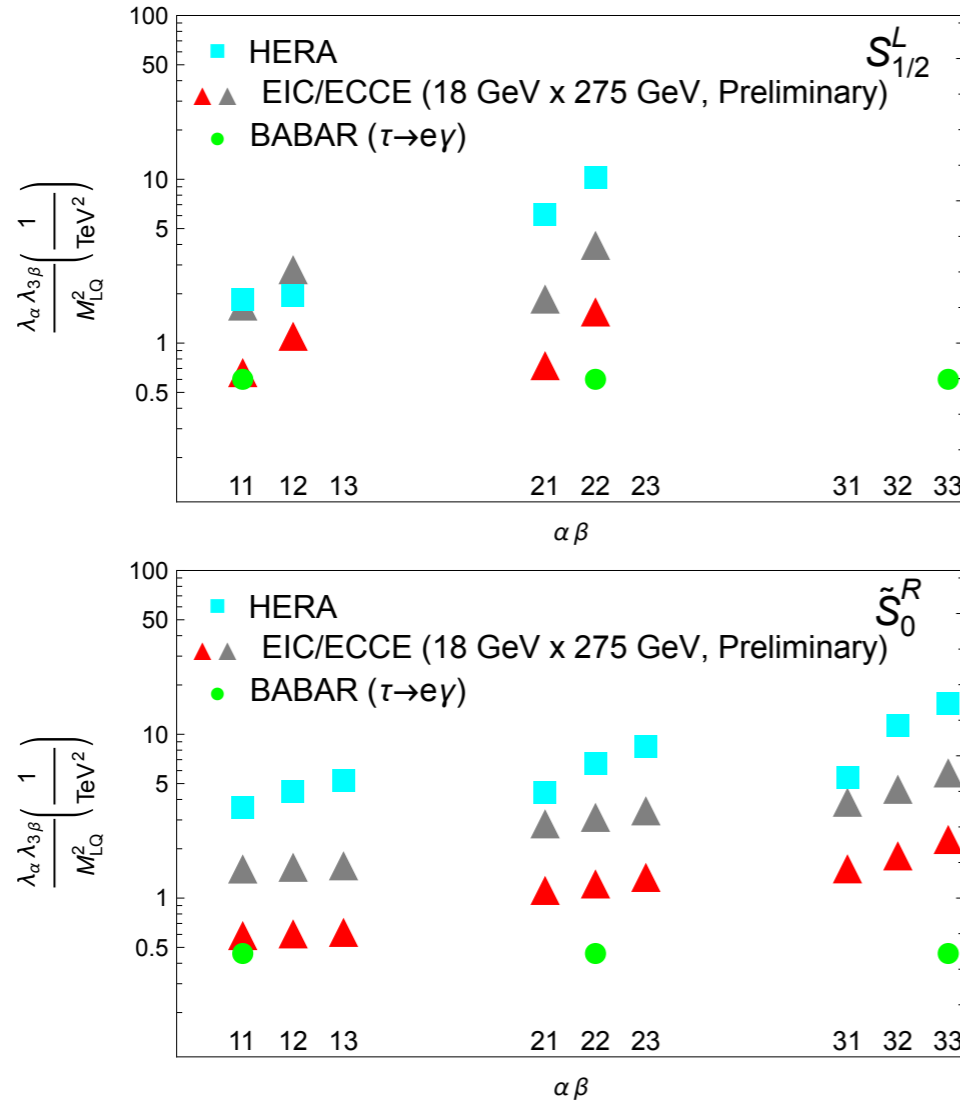


Figure 7: Limits on the scalar leptoquarks with $F = 0$ $S_{1/2}^L$ (top) and $|F| = 2 \tilde{S}_0^R$ (bottom) from 100 fb^{-1} of ep $18 \times 275 \text{ GeV}$ data, based on a sensitivity to leptoquark-mediated $ep \rightarrow \tau X$ cross section of size 1.7 fb (red triangles) or 11.4 fb (grey triangles) with ECCE. Note that due to small value of \sqrt{s} , EIC cannot constraint the third generation couplings of $S_{1/2}^L$ to top quarks. Limits from HERA [11, 5, 12, 6] are shown as cyan solid squares, and limits from $\tau \rightarrow e\gamma$ decays [3] are shown as green solid circles.

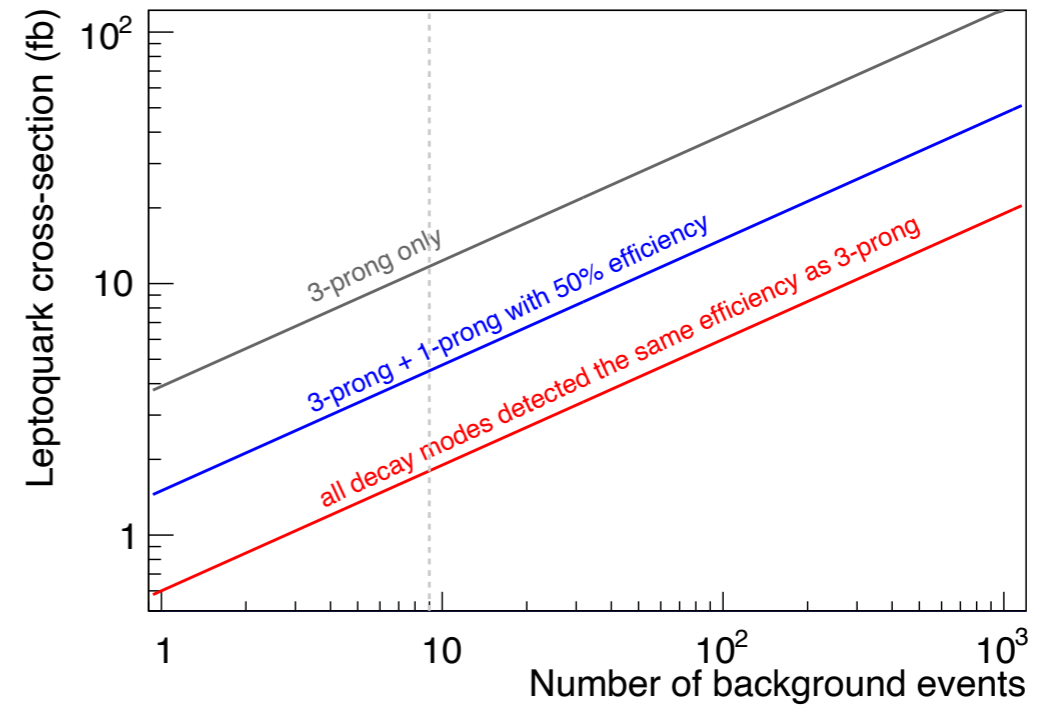


Figure 6: Cross section sensitivity for leptoquark search vs number of residual background events for 100 fb^{-1} integrated luminosity. The grey line corresponds to the scenario that only “3-prong” decay modes are detected. The blue line corresponds to the scenario where electron and pion “1-prong” decay modes could be detected with 50% efficiency of the “3-prong” case. And the red line shows the scenario if all decay modes were detected at the same efficiency as the “3-prong” case.

Conclusions

- The EIC is primarily a QCD machine.
- However, the EIC can also constrain BSM and be complementary to LHC searches and constraints from other low energy experiments:

- Precision measurements of the electroweak parameters
 - Leptophobic Z'
 - Dark Photon
 - Dark Z
- SMEFT Analysis to Constrain BSM
- Charged Lepton Flavor Violation

- Such a program physics is facilitated by:

- high luminosity
- wide kinematic range
- range of nuclear targets
- polarized beams
- Variety of observables

